BUCKLING OF MULTILAYER PLATES

BY FINITE ELEMENTS

By

HARRY RICHARD LUNDGREN

Bachelor of Science
in Civil Engineering
Purdue University
West Lafayette, Indiana
1950

Master of Science
Arizona State University
Tempe, Arizona
1962

Submitted to the faculty of the Graduate College
of the Oklahoma State University
in partial fulfillment of the requirements
for the degree of
DOCTOR OF PHILOSOPHY
May, 1967

BUCKLING OF MULTILAYER PLATES

BY FINITE ELEMENTS

Thesis Approved:

Alvin D. Salama
Thesis Adviser

Thomas Scott Dean

M N Reddy

R. E. Gaudy Jr.

D. D. Durham
Dean of the Graduate School

ACKNOWLEDGEMENT

The author wishes to express his gratitude and sincere appreciation to the following individuals and organizations:

To Professor Jan J. Tuma for his inspirational teaching and guidance;

To Professor Ahmed E. Salama for his advice and friendship in the preparation of this thesis;

To the members of the advisory committee, Professors Thomas S. Dean, Anthony F. Gaudy, Jr., Muppid N. Reddy and Ahmed E. Salama for their encouragement and help throughout the author's program;

To the staffs of the University Library and University Computer Center for assistance in the use of their facilities;

To the National Science Foundation and the Ford Foundation for their financial assistance;

To his wife, Joyce, for her understanding, encouragement, and assistance;

To Mrs. Jon M. Prescott, who typed the manuscript.

Harry Richard Lundgren

May, 1967
Stillwater, Oklahoma

TABLE OF CONTENTS

LIST OF TABLES

LIST OF FIGURES

NOMENCLATURE

The following symbols have been adopted for use in the thesis:

A, B, C, D	Classifications of boundary conditions;
a, b	Plate dimensions;
E_i	Modulus of elasticity of i^{th} membrane layer;
G_j	Modulus of rigidity of j^{th} core layer;
h_j	Thickness of j^{th} core layer;
i	Index, designates i^{th} membrane layer;
j	Index, designates j^{th} core layer;
M_x, M_y, M_{xy}	Moment stress resultants;
m	Total number of core layers;
n	Total number of membrane layers;
Q_x, Q_y	Transverse shear stress resultants;
T	Total plate thickness;
T_c	Dimension to core layer extremities;
t_i	Thickness of i^{th} membrane layer;
U	Strain energy;
$\bar{u}, \bar{v}, w$	Displacements;
V	Potential energy;
W	External work;
x, y, z	Coordinates;
z_i	Distance measured from the weighted neutral surface to the middle plane of the i^{th} membrane layer;

z_j . . . . . Distance measured from the centroidal surface to the middle plane of the j^{th} core layer;

Π . . . . . Total complementary energy;

α . . . . . Coefficients of displacement function assumed for bending stiffness;

β . . . . . Coefficients of stress functions assumed for bending stiffness modifier;

γ . . . . . Shear strain;

ϵ . . . . . Extensional strain;

η_1, η_2, η_3 . . . . . Plate property relationships;

θ . . . . . Rotation;

λ_1, λ_2 . . . . . Plate property relationships;

ν_i . . . . . Poisson's ratio for i^{th} membrane layer;

ρ . . . . . Coefficients of stress functions assumed for in-plane stiffness;

$\sigma_{x_i}, \sigma_{y_i}$ . . . . . Normal stresses at the i^{th} membrane layer;

τ_{xy_i} . . . . . In-plane shear stress at i^{th} membrane layer;

τ_{xz_j}, τ_{yz_j} . . . . . Transverse shear stresses at j^{th} core layer.

CHAPTER I

INTRODUCTION

1.1 Background

The development of sandwich plate theory and finite element investigations provides the background for the content of this thesis.

The connotation of sandwich plate as used here, and as generally understood, is a plate composed of three layers. The interior layer provides resistance to transverse shear only, while the exterior layers resist bending and twisting moments in the form of in-plane forces.

Multilayer plates are generally, although not always, considered to be constructed of several layers whose properties alternate. The alternating properties coincide with those described for sandwich plates.

The early theoretical work in this field was done by Reissner (1, 2), Hoff (3) and Eringen (4). One other article of particular interest is by Kuenzi, Norris, and Jenkinsen (5).

Reissner (2) demonstrated that the transverse normal stress contribution can be neglected in solving sandwich plates. He also developed an expression defining the valid region of his "small deflection" theory. Hoff (3) used a variational technique for solving both bending and buckling problems. Eringen (4) included the

possibility of thick facings and hence did not neglect the bending stiffness of each individual layer. Subsequent papers considered orthotropy.

The primary limitation of these papers and those that follow is that solutions are only available for a few boundary or support conditions.

The solution presented here is not based on any particular layer arrangement. It can, in fact, accommodate superimposed or overlapping layers, or as in the case of a homogeneous plate, all layers may have identical properties.

Previous work on multilayer plates has been done by Liaw (6) and Wong (7). Both of these papers applied variational techniques to develop the system of governing differential equations. Examples were solved for simply supported boundary conditions.

Pomazi (8) presented results for simply-supported multilayer plates. He solved Bolotin's (9) equilibrium equations by finite differences.

The concept of using finite elements to solve structures and mechanics problems has a rather vague origin. Because the slope-deflection method can really be categorized as a "finite element method" it could be considered as the beginning. However, as now used the "finite element method" usually pertains to plate, shell, and compound structures and in this form is of rather recent vintage. In 1956 Turner, et al (10) presented what is probably most appropriately considered the cornerstone of the current technique. Following papers by Melosh (11, 12), Best (13), Pian (14, 15), Zienkiewicz and Cheung (16), and

Severn and Taylor (17) refined and expanded the method but did not alter the original concept.

1.2 Finite Element Method

The basic premise of the method is that the structure is subdivided into a number of elements. The properties of the materials being known, the behavior characteristics of the elements can be determined. Now, with some variation depending upon the particular method being employed, the stiffnesses of the neighboring elements can be related through the generalized coordinates and forces at the nodes. Finally the elements are assembled to represent a structure as nearly like the original as possible. The problem becomes one of satisfying equilibrium and compatibility of the element, both internally and externally. The difference between this method and other approximate methods now becomes apparent. Wherein the other methods are applied to the governing differential equations and the approximations are mathematical, the finite element method provides an exact solution of a mathematical model which is an approximation of the real structure. If the model behaves exactly like the real structure, then an "exact" solution can be achieved. This is so in the case of beams and the slope-deflection method. In more complex structures this exact representation is generally not possible.

The successful construction of this mathematical model will permit the solution of many problems not solvable by existing methods. In addition to a variety of boundary conditions some discontinuity conditions can be handled.

There are two basic finite element methods by which stiffness of an element can be obtained. Either a displacement function or a stress function can be assumed. The assumption of a displacement function as the fundamental method imposes compatibility only. In this thesis both approaches are utilized. It is believed that the stress function provides greater accuracy and therefore is used in the determination of the bending stiffness. This development is presented in Chapter II. The use of a displacement function, however, is found to be much more direct for the determination of the stiffness modifying matrix in Chapter III, Section 1. The in-plane stiffness matrix in Chapter III, Section 2 utilizes a stress function.

Rectangular elements are used since only rectangular plates are to be considered.

1.3 Solution Procedure

Following are the steps in the determination of the critical stress of multilayered sandwich plates:

(a) Determine (or assume) the in-plane stress distribution;

(b) Determine the elemental bending stiffnesses;

(c) Determine the stiffness modifying matrix for each element reflecting the effect of the in-plane loads;

(d) Combine the elemental bending stiffness and elemental stiffness modifier;

(e) Assemble the modified elemental stiffnesses to obtain a total structure stiffness matrix;

(f) Apply boundary conditions and token lateral loads

and determine resulting deflections;

(g) Repeat prediction-correction procedure described in Chapter V to find critical stress.

1.4 Assumptions and Limitations

The layers designated as "membrane layers" have relatively high moduli of elasticity. They are considered to be sufficiently thin that the bending stiffness of the individual layer is negligible and the normal stress is a constant over the section. The layers designated as "core layers" are considered to have negligible normal stress stiffness. The method is applicable to orthotropic cores and membrane layers, although the presentation herein is for isotropic materials. The total plate thickness is considered to be sufficiently thin for the ordinary plate assumptions to be applicable. Hooke's Law is considered valid. Bond failures and local buckling will not be considered.

CHAPTER II

ELEMENTAL BENDING STIFFNESS

An element with four facing layers and three core layers is shown in Figures 1, 2, and 3 to illustrate the dimensions. Subscript i is associated throughout this thesis with the membrane layers, while j is associated with core layers. The thicknesses of the i^{th} membrane layer and j^{th} core layer are, respectively, t_i and h_j.

The neutral surface may be located such that

$$\sum_{i=1}^{n} \frac{E_i t_i z_i}{1 - \nu^2} = 0 \qquad (1)$$

where z_i is the distance from the neutral surface to the mid-plane of the membrane layers for n membrane layers.

The stresses on a typical layer are shown in Figure 4. The intensity of the in-plane stresses in the membrane layers, constant within any layer, varies linearly from the neutral surface. This is shown in Figure 5. The transverse shear stresses are assumed to be parabolically distributed across the section. The validity of this assumption requires relatively thin membrane layers and a fairly regular distribution of membrane and core layers since, as used here, the distribution of stresses across the section is independent of the in-plane stress distribution. This is approximately so for the aforementioned distribution. Figure 6 shows this distribution.

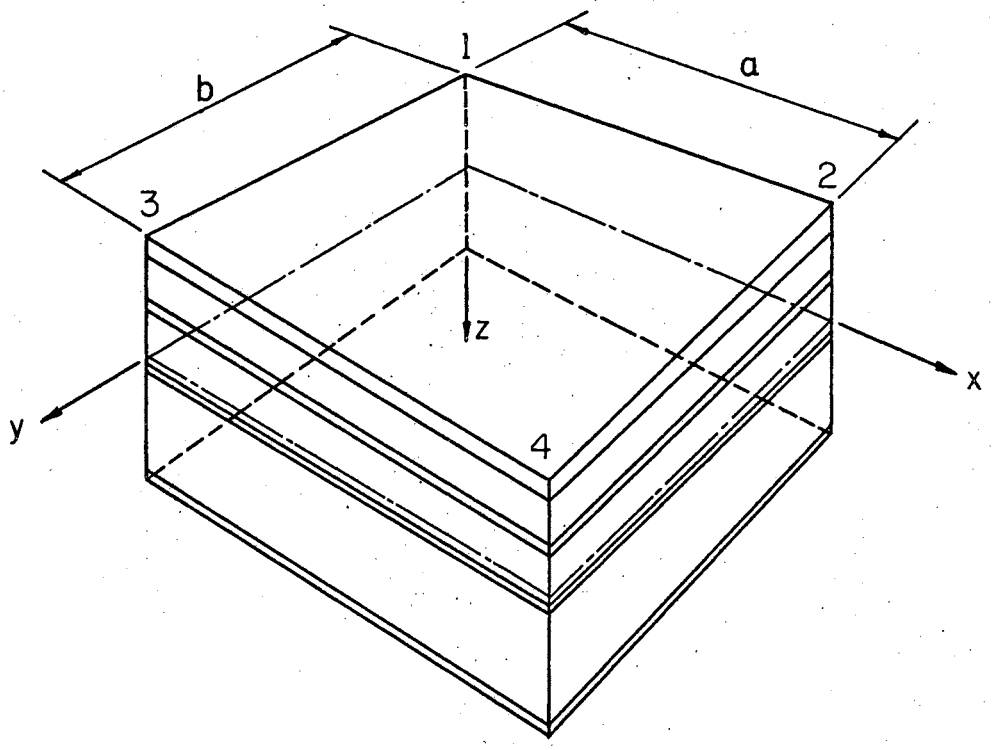

Figure 1. Dimensions and Axis Designation of Rectangular Element

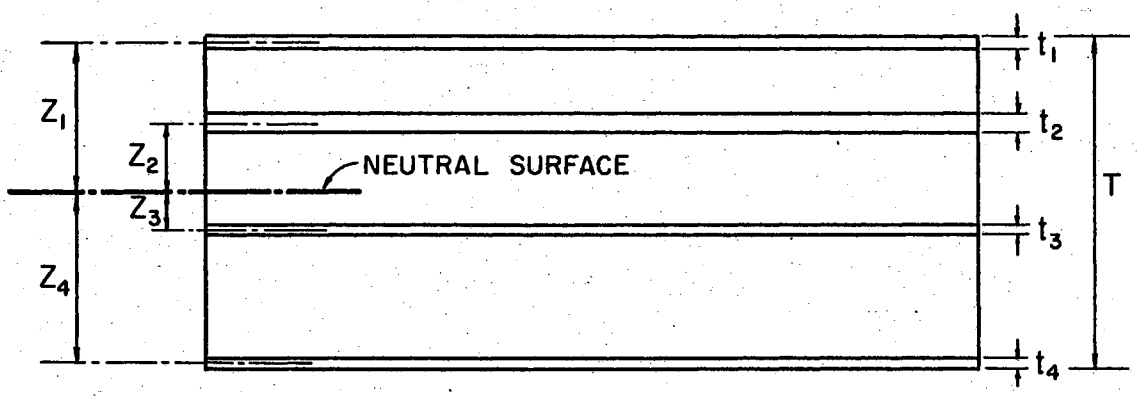

Figure 2. Membrane Layer Dimensions

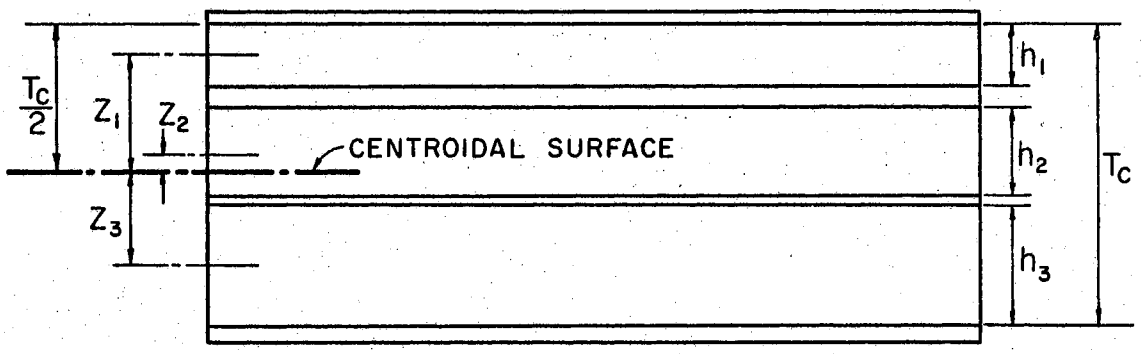

Figure 3. Core Layer Dimensions

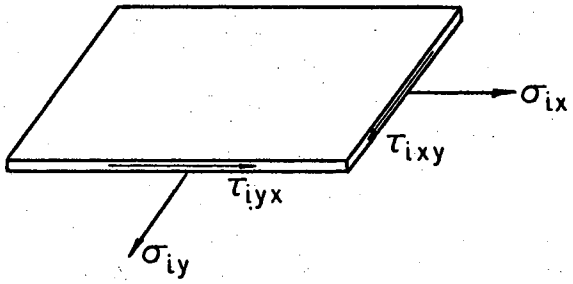

i th MEMBRANE LAYER

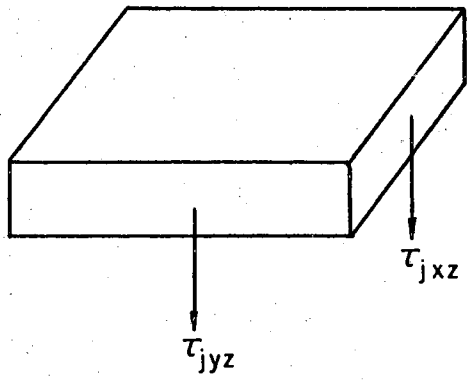

jth CORE LAYER

Figure 4. Stresses on Typical Layers

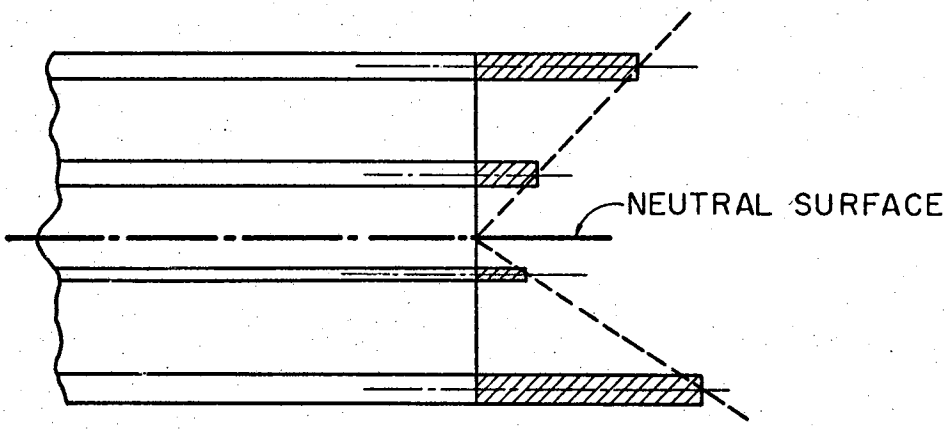

Figure 5. Membrane Stress Distribution

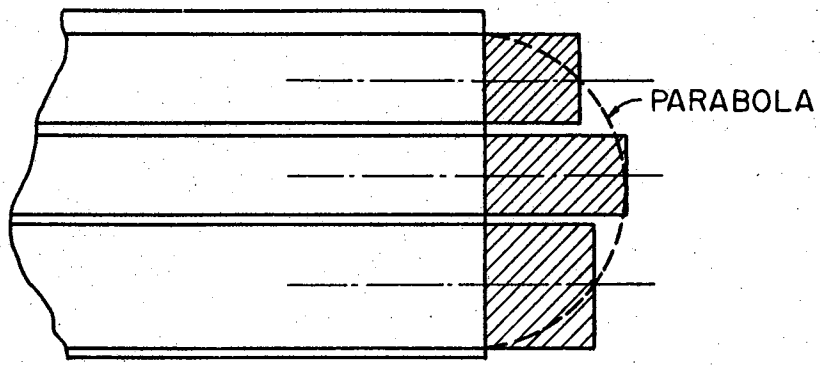

Figure 6. Core Layer Stress Distribution

So far only the stress distribution across the section has been considered. To describe the stress distribution in the xy plane a stress function is assumed. This stress function is of the same polynomial form as that used by Severn and Taylor (17) although containing additional terms to better define the distribution of the transverse shear stress. The resulting stress functions are

$$\sigma_{x_i} = \left[\beta_1 + \beta_2\bar{x} + \beta_3\bar{y} + \beta_4\bar{x}^2 + \beta_5\bar{x}\bar{y} + \beta_6\bar{y}^2 + \beta_{25}\bar{x}^3 + \beta_{26}\bar{x}^2\bar{y} + \beta_{27}\bar{x}\bar{y}^2 + \beta_{28}\bar{y}^3\right]\frac{8z_i}{T} \tag{2}$$

$$\sigma_{y_i} = \left[\beta_7 + \beta_8\bar{x} + \beta_9\bar{y} + \beta_{10}\bar{x}^2 + \beta_{11}\bar{x}\bar{y} + \beta_{12}\bar{y}^2 + \beta_{29}\bar{x}^3 + \beta_{30}\bar{x}^2\bar{y} + \beta_{31}\bar{x}\bar{y}^2 + \beta_{32}\bar{y}^3\right]\frac{8z_i}{T} \tag{3}$$

$$\tau_{xy_i} = \left[\beta_{13} + \beta_{14}\bar{x} + \beta_{15}\bar{y} + \beta_{16}\bar{x}^2 + \beta_{17}\bar{x}\bar{y} + \beta_{18}\bar{y}^2 + \beta_{33}\bar{x}^3 + \beta_{34}\bar{x}^2\bar{y} + \beta_{35}\bar{x}\bar{y}^2 + \beta_{36}\bar{y}^3\right]\frac{8z_i}{T} \tag{4}$$

$$\tau_{xz_j} = \left[\beta_{19} + \beta_{20}\bar{x} + \beta_{21}\bar{y} + \beta_{37}\bar{x}^2 + \beta_{38}\bar{x}\bar{y} + \beta_{39}\bar{y}^2\right]\left(1 - \frac{4z_j^2}{T_c}\right) \tag{5}$$

$$\tau_{yz_j} = \left[\beta_{22} + \beta_{23}\bar{x} + \beta_{24}\bar{y} + \beta_{40}\bar{x}^2 + \beta_{41}\bar{x}\bar{y} + \beta_{42}\bar{y}^2\right]\left(1 - \frac{4z_j^2}{T_c}\right) \tag{6}$$

where

$$\bar{x} = \frac{x}{a}$$

$$\bar{y} = \frac{y}{b}$$

T = total thickness of the plate

T_c = dimension from top of top core to bottom of bottom core layer

β_1 through β_{36} are constants.

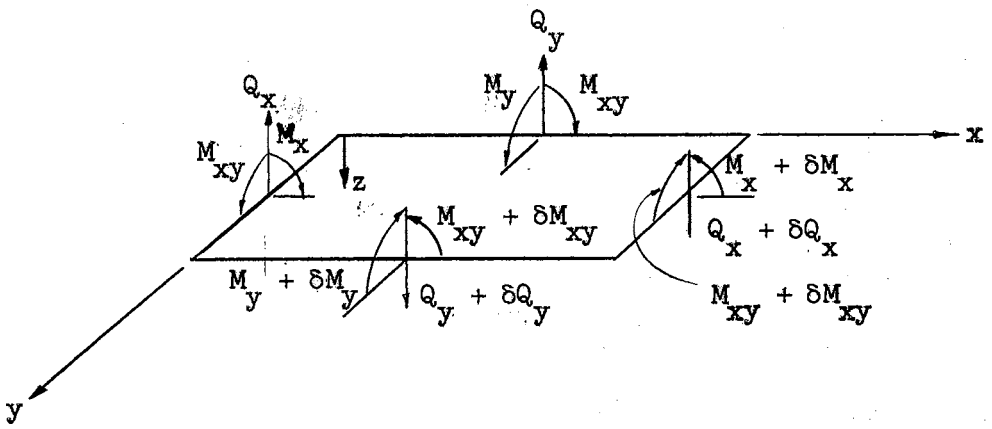

Figure 7. Elemental Edge Forces

From Figure 7 the equilibrium equations may be written as

$$\frac{\partial Q_x}{\partial x} + \frac{\partial Q_y}{\partial y} = 0 \tag{7}$$

$$\frac{\partial M_{xy}}{\partial x} + \frac{\partial M_y}{\partial y} - Q_y = 0 \tag{8}$$

$$\frac{\partial M_x}{\partial x} + \frac{\partial M_{xy}}{\partial y} - Q_x = 0 \tag{9}$$

Formulating the stress resultants:

$$M_x = \sum_{i=1}^{n} \sigma_{x_i} z_i t_i \tag{10}$$

$$M_y = \sum_{i=1}^{n} \sigma_{y_i} z_i t_i \tag{11}$$

$$M_{xy} = \sum_{i=1}^{n} \tau_{xy_i} z_i t_i \tag{12}$$

$$Q_x = \sum_{j=1}^{m} \tau_{xz_j} z_j t_j \tag{13}$$

$$Q_y = \sum_{j=1}^{m} \tau_{yz_j} z_j t_j \tag{14}$$

and substituting from equations (2) through (6) into equations (10) through (14) and thence into (7), (8) and (9) and introducing the following notation

$$\eta_1 = \sum_{j=1}^{m} \left(1 - \frac{4z_j^2}{T_c^2}\right) h_j \tag{15}$$

$$\eta_2 = \sum_{i=1}^{n} \left(\frac{8z_i^2}{T}\right) t_i \tag{16}$$

$$\eta_3 = \frac{\eta_2}{\eta_1} \tag{17}$$

the following relationships are established between the coefficients resulting in the elimination of fifteen of the original thirty-six coefficients.

$$\beta_{17} = -\frac{b}{a}\beta_4 - \frac{a}{b}\beta_{12} \tag{18a}$$

$$\beta_{19} = \eta_3 \left[\frac{2\beta_2}{a} + \frac{\beta_{15}}{b}\right] \tag{18b}$$

$$\beta_{20} = \eta_3 \left[\frac{2\beta_4}{a} + \frac{\beta_{17}}{b}\right] \tag{18c}$$

$$\beta_{21} = \eta_3 \left[\frac{\beta_5}{a} + \frac{2\beta_{18}}{b}\right] \tag{18d}$$

$$\beta_{22} = \eta_3 \left[\frac{\beta_9}{b} + \frac{\beta_{14}}{a}\right] \tag{18e}$$

$$\beta_{23} = \eta_3 \left[\frac{\beta_{11}}{b} + \frac{2\beta_{16}}{a}\right] \tag{18f}$$

$$\beta_{24} = \eta_3 \left[\frac{2\beta_{12}}{b} + \frac{\beta_{17}}{a}\right] \tag{18g}$$

$$\beta_{34} = -\frac{3b}{2a}\beta_{25} - \frac{a}{2b}\beta_{31} \tag{18h}$$

$$\beta_{35} = -\frac{b}{2a}\beta_{26} - \frac{3a}{2b}\beta_{32} \tag{18i}$$

$$\beta_{37} = \eta_3 \left[\frac{3}{a}\beta_{25} + \frac{\beta_{34}}{b}\right] \tag{18j}$$

$$\beta_{38} = \eta_3 \left[\frac{2}{a}\beta_{26} + \frac{2}{b}\beta_{35}\right] \tag{18k}$$

$$\beta_{39} = \eta_3 \left[\frac{\beta_{27}}{a} + \frac{3}{b}\beta_{36}\right] \tag{18l}$$

$$\beta_{40} = \eta_3 \left[\frac{\beta_{30}}{b} + \frac{3}{a}\beta_{33}\right] \tag{18m}$$

$$\beta_{41} = \eta_3 \left[\frac{2}{b}\beta_{31} + \frac{2}{a}\beta_{34}\right] \tag{18n}$$

$$\beta_{42} = \eta_3 \left[\frac{3}{b}\beta_{32} + \frac{\beta_{35}}{a}\right]. \tag{18o}$$

Substituting these relationships back into the stress expressions (2), (3), (4), (5), (6) yields:

$$\sigma_{x_i} = \lambda_2 \left[\beta_1 + \beta_2\bar{x} + \beta_3\bar{y} + \beta_4\bar{x}^2 + \beta_5\bar{x}\bar{y} + \beta_6\bar{y}^2 + \beta_{25}\bar{x}^3 + \beta_{26}\bar{x}^2\bar{y} + \beta_{27}\bar{x}\bar{y}^2 + \beta_{28}\bar{y}^3\right] \tag{19}$$

$$\sigma_{y_i} = \lambda_2 \left[\beta_7 + \beta_8\bar{x} + \beta_9\bar{y} + \beta_{10}\bar{x}^2 + \beta_{11}\bar{x}\bar{y} + \beta_{12}\bar{y}^2 + \beta_{29}\bar{x}^3 + \beta_{30}\bar{x}^2\bar{y} + \beta_{31}\bar{x}\bar{y}^2 + \beta_{32}\bar{y}^3\right] \tag{20}$$

$$\tau_{xy_i} = \lambda_2 \left[-\frac{b\bar{x}\bar{y}}{a}\beta_4 - \frac{a\bar{x}\bar{y}}{b}\beta_{12} + \beta_{13} + \beta_{14}\bar{x} + \beta_{15}\bar{y} + \beta_{16}\bar{x}^2 + \beta_{18}\bar{y}^2 - \frac{3b\bar{x}^2\bar{y}}{2a}\beta_{25} - \frac{b\bar{x}\bar{y}^2}{2a}\beta_{26} - \frac{a\bar{x}^2\bar{y}}{2b}\beta_{31} - \frac{3a\bar{x}\bar{y}^2}{2b}\beta_{32} + \beta_{33}\bar{x}^3 + \beta_{36}\bar{y}^3\right] \tag{21}$$

$$\tau_{xz_j} = \lambda_1\eta_3 \left[\frac{1}{a}\beta_2 + \frac{\bar{x}}{a}\beta_4 + \frac{\bar{y}}{a}\beta_5 - \frac{a\bar{x}}{b^2}\beta_{12} + \frac{1}{b}\beta_{15} + \frac{2\bar{y}}{b}\beta_{18} + \frac{3\bar{x}^2}{2a}\beta_{25} + \frac{\bar{x}\bar{y}}{a}\beta_{26} + \frac{\bar{y}^2}{a}\beta_{27} - \frac{a\bar{x}^2}{2b^2}\beta_{31} - \frac{3a\bar{x}\bar{y}}{b^2}\beta_{32} + \frac{3\bar{y}^2}{b}\beta_{36}\right] \tag{22}$$

$$\tau_{yz_j} = \lambda_1\eta_3 \left[-\frac{b\bar{y}}{a^2}\beta_4 + \frac{1}{b}\beta_9 + \frac{\bar{x}}{b}\beta_{11} + \frac{\bar{y}}{b}\beta_{12} + \frac{1}{a}\beta_{14} + \frac{2\bar{x}}{a}\beta_{16} - \frac{3b\bar{x}\bar{y}}{a^2}\beta_{25} - \frac{b\bar{y}^2}{2a^2}\beta_{26} + \frac{\bar{x}^2}{b}\beta_{30} + \frac{\bar{x}\bar{y}}{b}\beta_{31} + \frac{3\bar{y}^2}{2b}\beta_{32} + \frac{3\bar{x}^2}{a}\beta_{33}\right] \tag{23}$$

where

$$\lambda_1 = 1 - \frac{4z_i^2}{T_c^2} \tag{24}$$

$$\lambda_2 = \frac{8z_i}{T} \, . \tag{25}$$

These equations can be expressed in matrix form as

$$[\sigma] = [P][\beta] \tag{26}$$

where

$$[\sigma] = \left\{\sigma_{x_i} \; \sigma_{y_i} \; \tau_{xy_i} \; \tau_{xz_j} \; \tau_{yz_j}\right\}$$

$$[\beta] = \left\{\beta_1 \; \beta_2 \; \beta_3 \; \beta_4 \; \beta_5 \; \beta_6 \; \beta_7 \; \beta_8 \; \beta_9 \right.$$
$$\beta_{10} \; \beta_{11} \; \beta_{12} \; \beta_{13} \; \beta_{14} \; \beta_{15} \; \beta_{16} \; \beta_{18} \; \beta_{25}$$
$$\left. \beta_{26} \; \beta_{27} \; \beta_{28} \; \beta_{29} \; \beta_{30} \; \beta_{31} \; \beta_{32} \; \beta_{33} \; \beta_{36}\right\}$$

and $[P]$ is a coefficient matrix containing algebraic terms in $\bar{x}$ and $\bar{y}$.

The internal strain energy can be formulated in matrix form as

$$U = \frac{1}{2} \int_V [\sigma] \, [\epsilon] \, dv \, . \tag{27}$$

For the required finite summation of the layers this formulation becomes

$$U = \frac{1}{2} \int_A \sum_T [\sigma][\epsilon] \, z_{i,j} \, dA \tag{28}$$

in which $\sum_T \cdots z_{i,j}$ indicates summation over both core and membrane layers.

Letting

$$[N] = \begin{bmatrix} \frac{1}{E_i} & -\frac{\nu_i}{E_i} & 0 & 0 & 0 \\ -\frac{\nu}{E_i} & \frac{1}{E_i} & 0 & 0 & 0 \\ 0 & 0 & \frac{\bar{\nu}}{E_i} & 0 & 0 \\ 0 & 0 & 0 & \frac{1}{G_j} & 0 \\ 0 & 0 & 0 & 0 & \frac{1}{G_j} \end{bmatrix}$$

where

$$\bar{\nu} = 2(1 + \nu)$$

and

$$[\epsilon] = \left\{ \epsilon_x \quad \epsilon_y \quad \gamma_{xy} \quad \gamma_{xz} \quad \gamma_{yz} \right\},$$

it follows from the stress-strain relationship given by

$$[\epsilon] = [N][\sigma] \tag{29}$$

that

$$U = \frac{1}{2} \int_A \sum_T [\sigma]^T [N][\sigma] \, z_{i,j} \, dA \, . \tag{30}$$

It should be noted at this point that it would be possible to provide a solution to plates with orthotropic cores and membrane layers by using E_{x_i}, E_{y_i}, V_{x_i}, V_{y_i}, G_{x_j}, and G_{y_j} in [N]. This has not been done in the present solution, therefore it is limited to isotropic layers. Each layer may have different properties, however.

Utilizing equation (26) and its transpose, the strain energy can now be expressed

$$U = \frac{1}{2}\int_A \sum_T [\beta]^T [P]^T [N][P][\beta]\, z_{i,j}\, dA \tag{31}$$

which may be rewritten in the form

$$U = \frac{1}{2}[\beta]^T [H][\beta] \tag{32}$$

in which

$$[H] = \int_A \sum_T [P]^T [N][P]\, z_{i,j}\, dA\ . \tag{33}$$

Performing the indicated integrations and summation, the [H] matrix can be formed.

$$[H] = \sum_{i=1}^{n} \sum_{j=1}^{m} \begin{bmatrix} H_{11} & H_{12} \\ H_{21} & H_{22} \end{bmatrix}$$

in which

$[H_{11}]$ is shown in Figure 8a,

$[H_{12}]$ is shown in Figure 8b,

$[H_{22}]$ is shown in Figure 8c,

$[H_{21}]$ is equal to the transpose of $[H_{12}]$.

Next, an expression for the external energy of the element is developed. The total work done by the forces acting on the surface of the element is given by

$$W = \oint [S][u]\, ds \tag{34}$$

where [S] and [u] are, respectively, the forces and displacements at the edge of the element. The positive directions of the edge forces are shown in Figure 9.

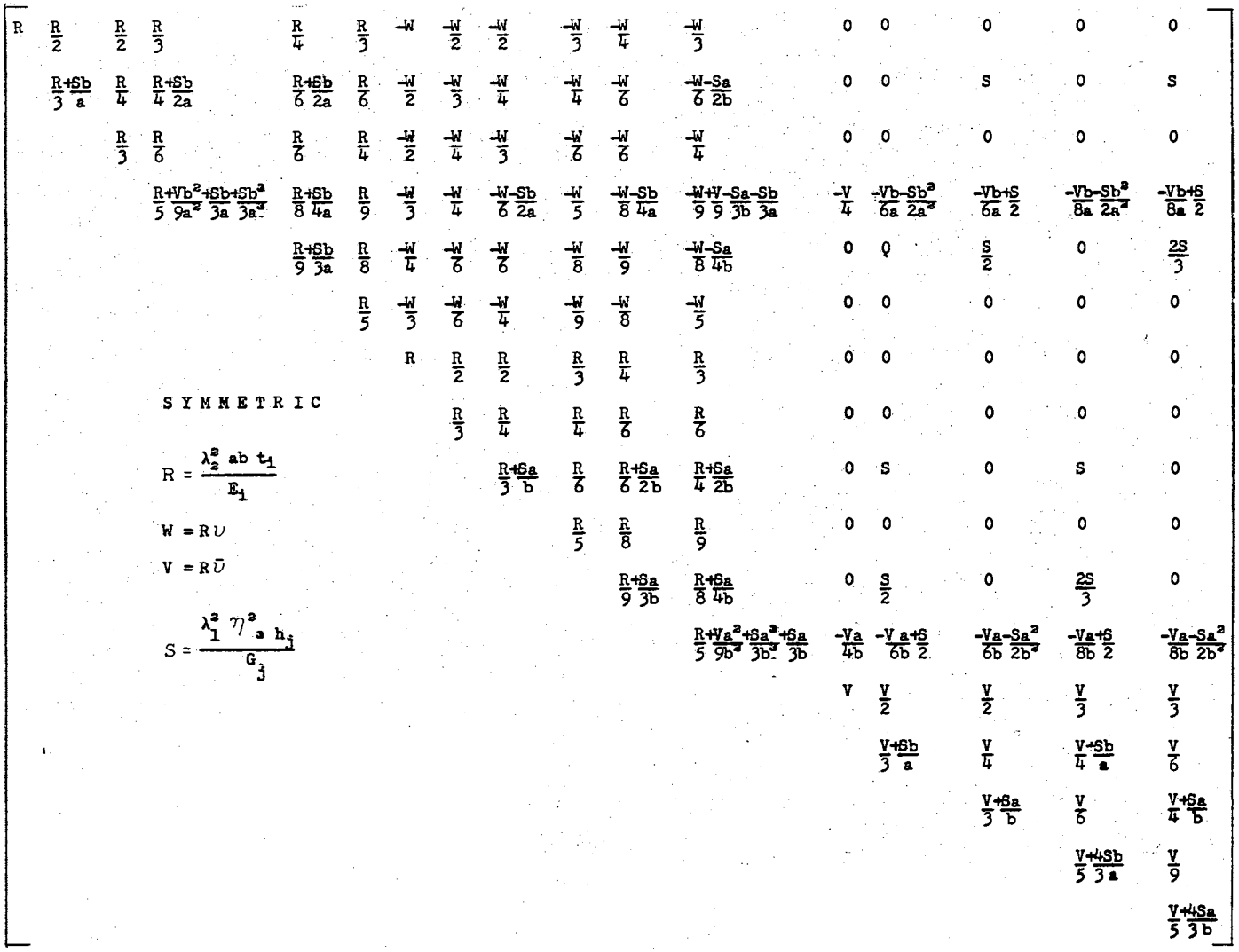

Figure 8a. Sub-matrix $[H_{11}]$

$$
\begin{bmatrix}
\frac{R}{4} & \frac{R}{6} & \frac{R}{6} & \frac{R}{4} & \frac{-W}{4} & \frac{-W}{6} & \frac{-W}{4} & \frac{-W}{6} & 0 & 0 \\
\frac{R+Sb}{5\ 2a} & \frac{R+Sb}{8\ 4a} & \frac{R+Sb}{9\ 3a} & \frac{R}{8} & \frac{-W}{5} & \frac{-W}{8} & \frac{-W-Sa}{9\ 6b} & \frac{-W-3Sa}{8\ 4b} & 0 & S \\
\frac{R}{8} & \frac{R}{9} & \frac{R}{8} & \frac{R}{5} & \frac{-W}{8} & \frac{-W}{9} & \frac{-W}{8} & \frac{-W}{5} & 0 & 0 \\
\frac{R+Vb^2+3Sb+Sb^3}{6\ 8a^2\ 8a\ 2a^3} & \frac{R+Vb^2+Sb+Sb^3}{10\ 24a^2\ 6a\ 8a^3} & \frac{R+Sb}{12\ 6a} & \frac{R}{12} & \frac{-W}{6} & \frac{-W-Sb}{10\ 6a} & \frac{-W+V-Sa-Sb}{12\ 24\ 8b\ 6a} & \frac{-W+V-Sa-3Sb}{12\ 8\ 2b\ 8a} & \frac{-Vb-Sb^2}{10a\ 2a^2} & \frac{-Vb+S}{10a\ 2} \\
\frac{R+1\ Sb}{10\ 4\ a} & \frac{R+Sb}{12\ 6a} & \frac{R+Sb}{12\ 4a} & \frac{R}{10} & \frac{-W}{10} & \frac{-W}{12} & \frac{-W-Sa}{12\ 12b} & \frac{-W-Sa}{10\ 2b} & 0 & \frac{3S}{4} \\
\frac{R}{12} & \frac{R}{12} & \frac{R}{10} & \frac{R}{6} & \frac{-W}{12} & \frac{-W}{12} & \frac{-W}{10} & \frac{-W}{6} & 0 & 0 \\
\frac{-W}{4} & \frac{-W}{6} & \frac{-W}{6} & \frac{-W}{4} & \frac{R}{4} & \frac{R}{6} & \frac{R}{6} & \frac{R}{4} & 0 & 0 \\
\frac{-W}{5} & \frac{-W}{8} & \frac{-W}{9} & \frac{-W}{8} & \frac{R}{5} & \frac{R}{8} & \frac{R}{9} & \frac{R}{8} & 0 & 0 \\
\frac{-W-3Sb}{8\ 4\ a} & \frac{-W-Sb}{9\ 6a} & \frac{-W}{8} & \frac{-W}{5} & \frac{R}{8} & \frac{R+Sa}{9\ 3b} & \frac{R+Sa}{8\ 4b} & \frac{R+Sa}{5\ 2b} & S & 0 \\
\frac{-W}{6} & \frac{-W}{10} & \frac{-W}{12} & \frac{-W}{12} & \frac{R}{6} & \frac{R}{10} & \frac{R}{12} & \frac{R}{12} & 0 & 0 \\
\frac{-W-Sb}{10\ 2a} & \frac{-W-Sb}{12\ 12a} & \frac{-W}{12} & \frac{-W}{10} & \frac{R}{10} & \frac{R+Sa}{12\ 4b} & \frac{R+Sa}{12\ 6b} & \frac{R+Sa}{10\ 4b} & \frac{3S}{4} & 0 \\
\frac{-W+V-3Sa-Sb}{12\ 8\ 8b\ 2a} & \frac{-W+V-Sa-Sb}{12\ 24\ 6b\ 8a} & \frac{-W-Sa}{10\ 6b} & \frac{-W}{6} & \frac{R}{12} & \frac{R+Sa}{12\ 6b} & \frac{R+Va^2+Sa^3+Sa}{10\ 24b^2\ 8b^3\ 6b} & \frac{R+Va^2+Sa^3+3Sa}{6\ 8b^2\ 2b^3\ 8b} & \frac{-Va+S}{10b\ 2} & \frac{-Va-Sa^2}{10b\ 2b^2} \\
\frac{-Vb}{4a} & \frac{-Vb}{12a} & 0 & 0 & 0 & 0 & \frac{-Va}{12b} & \frac{-Va}{4b} & \frac{V}{4} & \frac{V}{4} \\
\frac{-3\ Vb-3Sb^2}{16\ a\ 4\ a^2} & \frac{-Vb-Sb^2}{18a\ 6a^2} & 0 & 0 & 0 & \frac{S}{3} & \frac{-Va+S}{16b\ 4} & \frac{-Va+S}{6b\ 2} & \frac{V+Sb}{5\ a} & \frac{V}{8} \\
\frac{-Vb+S}{6a\ 2} & \frac{-Vb+S}{16a\ 4} & \frac{S}{3} & 0 & 0 & 0 & \frac{-Va-Sa^2}{18b\ 6b^2} & \frac{-3Va-3Sa^2}{16b\ 4b^2} & \frac{V}{8} & \frac{V+Sa}{5\ b} \\
\frac{-3\ Vb-Sb^2}{20\ a\ a^2} & \frac{-Vb-Sb^2}{24a\ 6a^2} & 0 & 0 & 0 & \frac{S}{2} & \frac{-Va+S}{20b\ 3} & \frac{-Va+S}{8b\ 2} & \frac{V+3Sb}{6\ 2a} & \frac{V}{12} \\
\frac{-Vb+S}{8a\ 2} & \frac{-Vb+S}{20a\ 3} & \frac{S}{2} & 0 & 0 & 0 & \frac{-Va-Sa^2}{24b\ 6b^2} & \frac{-3Va-Sa^2}{20b\ b^2} & \frac{V}{12} & \frac{V+3Sa}{6\ 2b}
\end{bmatrix}
$$

Figure 8b. Sub-matrix $[H_{12}]$

$$
\begin{bmatrix}
\frac{R}{7}+\frac{3Vb^2}{20a}+\frac{9Sb}{20a}+\frac{Sb^3}{a^3} & \frac{R}{12}+\frac{3Vb^2}{64a^2}+\frac{3}{16}\frac{Sb}{a}+\frac{3Sb^3}{16a^3} & \frac{R}{15}+\frac{Sb}{6a} & \frac{R}{16} & \frac{-W}{7} & \frac{-W}{12}-\frac{3Sb}{8a} & \frac{-W}{15}+\frac{V}{20}-\frac{3Sa}{20b}-\frac{Sb}{3a} & \frac{-W}{16}+\frac{9V}{64}-\frac{9Sa}{16b}-\frac{9Sb}{16a} & \frac{-Vb}{8a}-\frac{9Sb^2}{8a^2} & \frac{-Vb}{10a}+\frac{S}{2} \\
 & \frac{R}{15}+\frac{Vb^2}{60a^2}+\frac{Sb}{9a}+\frac{Sb^3}{20a^3} & \frac{R}{16}+\frac{Sb}{8a} & \frac{R}{15} & \frac{-W}{12} & \frac{-W}{15}-\frac{Sb}{18a} & \frac{-W}{16}+\frac{V}{64}-\frac{Sa}{16b}-\frac{Sb}{16a} & \frac{-W}{15}+\frac{V}{20}-\frac{Sa}{3b}-\frac{3Sb}{20a} & \frac{-Vb}{30a}-\frac{Sb^2}{6a^2} & \frac{-Vb}{24a}+\frac{3S}{8} \\
 & & \frac{R}{15}+\frac{Sb}{5a} & \frac{R}{12} & \frac{-W}{15} & \frac{-W}{16} & \frac{-W}{15}-\frac{Sa}{18b} & \frac{-W}{12}-\frac{3Sa}{8b} & 0 & \frac{3S}{5} \\
 & & & \frac{R}{7} & \frac{-W}{16} & \frac{-W}{15} & \frac{-W}{12} & \frac{-W}{7} & 0 & 0 \\
 & & & & \frac{R}{7} & \frac{R}{12} & \frac{R}{15} & \frac{R}{16} & 0 & 0 \\
 & & & & & \frac{R}{15}+\frac{Sa}{5b} & \frac{R}{16}+\frac{Sa}{8b} & \frac{R}{15}+\frac{Sa}{6b} & \frac{3S}{5} & 0 \\
 & \text{SYMMETRICAL} & & & & & \frac{R}{15}+\frac{Va^2}{60b^2}+\frac{Sa^3}{20b^3}+\frac{Sa}{9b} & \frac{R}{12}+\frac{3Va^2}{64b^2}+\frac{3Sa^3}{16b^3}+\frac{3Sa}{16b} & \frac{-Va}{24b}+\frac{3S}{8} & \frac{-Va}{30b}-\frac{Sa^2}{6b^2} \\
 & & & & & & & \frac{R}{7}+\frac{3Va^2}{20b^2}+\frac{Sa^3}{8^3}+\frac{9Sa}{20b} & \frac{-Va}{10b}+\frac{S}{2} & \frac{-Va}{8b}-\frac{9Sa^2}{8b^3} \\
 & & & & & & & & \frac{V}{7}+\frac{9Sb}{5a} & \frac{V}{16} \\
 & & & & & & & & & \frac{V}{7}+\frac{9Sa}{5b}
\end{bmatrix}
$$

Figure 8c. Sub-matrix $[H_{22}]$

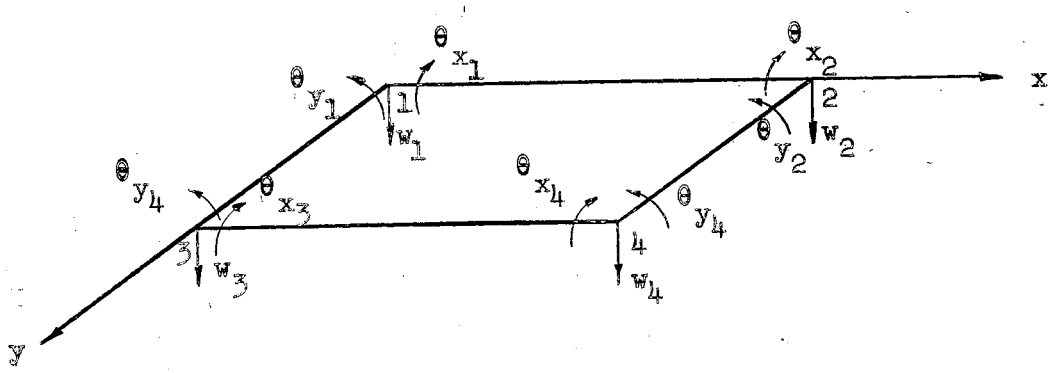

Figure 9. Nodal Displacements

In order to determine [u] an edge displacement function is assumed for each edge of the element

$$w_{kl} = A_{kl0} + A_{kl1}x + A_{kl2}x^2 + A_{kl3}x^3$$

in which k and l are the nodes at the ends of the element edge. The constants A_{kl} can be determined in terms of the generalized displacements [q], where

$$[q] = \{\theta_{x_1} \quad \theta_{y_1} \quad w_1 \quad \theta_{x_2} \quad \theta_{y_2} \quad w_2 \quad \theta_{x_3} \quad \theta_{y_3} \quad w_3 \quad \theta_{x_4} \quad \theta_{y_4} \quad w_4\} \tag{35}$$

and are shown on Figure 9 in their positive directions. For any given edge the constants are a function of the adjacent nodal displacements

and the tangential slope (parallel to the element edge) evaluated at the nodes. Since the resulting equation expresses the displacement of the element edge in terms of the nodal displacements and since the nodal displacements of two bordering elements are identical, then compatibility of displacement and of the tangential slope are assured at the common boundary. In addition, a linear normal slope (perpendicular to the element edge) is assumed between node points. This causes compatibility to be satisfied with regard to the normal slopes of the adjacent elements although the linearization of the variation introduces an approximation.

These relationships can be formulated in matrices as follows

$$[u] = [L][q] \ . \tag{36}$$

The moments and forces on the element edge can be derived from the stress resultants developed earlier (equations (10) through (14)) thus yielding

$$M_{y_{12}} = (M_y)_{y=0} = -\eta_2 \left[\beta_7 + \beta_8\bar{x} + \beta_{10}\bar{x}^2 + \beta_{29}\bar{x}^3\right] \tag{37a}$$

$$M_{xy_{12}} = (M_{xy})_{y=0} = -\eta_2 \left[\beta_{13} + \beta_{14}\bar{x} + \beta_{16}\bar{x}^2 + \beta_{33}\bar{x}^3\right] \tag{37b}$$

$$Q_{y_{12}} = (Q_y)_{y=0} = -\eta_2 \left[\frac{1}{b}\beta_9 + \frac{1}{a}\beta_{14} + \frac{\bar{x}}{b}\beta_{11} + \frac{2\bar{x}}{a}\beta_{16} + \frac{\bar{x}^2}{b}\beta_{30} + \frac{3\bar{x}^2}{a}\beta_{33}\right] \tag{37c}$$

$$M_{xy_{24}} = (M_{xy})_{x=a} = \eta_2 \left[\beta_{13} + \beta_{14} + \beta_{15}\bar{y} + \beta_{16} - \frac{b\bar{y}}{a}\beta_4 - \frac{a\bar{y}}{b}\beta_{12} + \beta_{18}\bar{y}^2 + \beta_{33}\right.$$

$$- \frac{3b\bar{y}}{2a}\beta_{25} - \frac{a\bar{y}}{2b}\beta_{31} - \frac{b\bar{y}^2}{2a}\beta_{26}$$

$$- \frac{3a\bar{y}^2}{2b}\beta_{32} + \beta_{36}\bar{y}^3\Big] \qquad (37d)$$

$$M_{x_{24}} = (M_x)_{x=a} = \eta_2\Big[\beta_1 + \beta_2 + \beta_3\bar{y} + \beta_4 + \beta_5\bar{y} + \beta_6\bar{y}^2$$

$$+ \beta_{25} + \beta_{26}\bar{y} + \beta_{27}\bar{y}^2 + \beta_{28}\bar{y}^3\Big] \qquad (37e)$$

$$Q_{x_{24}} = (Q_x)_{x=a} = \eta_2\Big[\frac{1}{a}\beta_2 + \frac{1}{a}\beta_4 + \frac{\bar{y}}{a}\beta_5 - \frac{a}{b^2}\beta_{12}$$

$$+ \frac{1}{b}\beta_{15} + \frac{1}{b}\beta_{17} + \frac{2\bar{y}}{b}\beta_{18}$$

$$+ \frac{3}{2a}\beta_{25} + \frac{\bar{y}}{a}\beta_{26} + \frac{\bar{y}^2}{a}\beta_{27}$$

$$- \frac{a}{2b^2}\beta_{31} - \frac{3a\bar{y}}{b^2}\beta_{32} + \frac{3\bar{y}^2}{b}\beta_{36}\Big] \qquad (37f)$$

$$M_{y_{34}} = (M_y)_{y=b} = \eta_2\Big[\beta_7 + \beta_8\bar{x} + \beta_9 + \beta_{10}\bar{x}^2 + \beta_{11}\bar{x} + \beta_{12}$$

$$+ \beta_{29}\bar{x}^3 + \beta_{30}\bar{x}^2 + \beta_{31}\bar{x} + \beta_{32}\Big] \qquad (37g)$$

$$M_{xy_{34}} = (M_{xy})_{y=b} = \eta_2\Big[\beta_{13} + \beta_{14}\bar{x} + \beta_{15} + \beta_{16}\bar{x}^2 - \frac{b\bar{x}}{a}\beta_4$$

$$- \frac{a\bar{x}}{b}\beta_{12} + \beta_{18} - \frac{3b\bar{x}^2}{2a}\beta_{25}$$

$$- \frac{b\bar{x}}{2a}\beta_{26} - \frac{a\bar{x}^2}{2b}\beta_{31} - \frac{3a\bar{x}}{2b}\beta_{32}$$

$$+ \beta_{33}\bar{x}^3 + \beta_{36}\Big] \qquad (37h)$$

$$Q_{y_{34}} = (Q_y)_{y=b} = \eta_2\Big[- \frac{b}{a^2}\beta_4 + \frac{1}{b}\beta_9 + \frac{\bar{x}}{b}\beta_{11} + \frac{1}{b}\beta_{12}$$

$$+ \frac{1}{a}\beta_{14} + \frac{2\bar{x}}{a}\beta_{16} - \frac{3b\bar{x}}{a^2}\beta_{25}$$

$$- \frac{b}{2a^2}\beta_{26} + \frac{\bar{x}^2}{b}\beta_{30} + \frac{\bar{x}}{b}\beta_{31}$$

$$+ \frac{3}{2b}\beta_{32} + \frac{3\bar{x}^2}{a}\beta_{33}\Big] \qquad (37i)$$

$$M_{xy_{13}} = (M_{xy})_{x=0} = -\eta_2\left[\beta_{13} + \beta_{15}\bar{y} + \beta_{18}\bar{y}^2 + \beta_{36}\bar{y}^3\right] \qquad (37j)$$

$$M_{x_{13}} = (M_x)_{x=0} = -\eta_2\left[\beta_1 + \beta_3\bar{y} + \beta_6\bar{y}^2 + \beta_{28}\bar{y}^3\right] \qquad (37k)$$

$$Q_{x_{13}} = (Q_x)_{x=0} = -\eta_2\left[\frac{1}{a}\beta_2 + \frac{\bar{y}}{a}\beta_5 + \frac{1}{b}\beta_{15}\right.$$

$$\left. + \frac{2\bar{y}}{b}\beta_{18} + \frac{\bar{y}^2}{a} + \frac{3\bar{y}^2}{b}\right] \qquad (37l)$$

The preceding equations may be arranged in matrix form as

$$[S] = [R][\beta] \, . \qquad (38)$$

Substituting equation (35) and equation (38) into equation (34) yields

$$W = \oint [\beta]^T [R]^T [L][q] \, ds \qquad (39)$$

which may be rewritten as

$$W = [\beta]^T [T][q] \qquad (40)$$

in which

$$[T] = \oint [R]^T [L] \, ds \, . \qquad (41)$$

The resulting T matrix is shown in Figure 10.

$$
\eta_2 \begin{bmatrix}
0 & -\frac{b}{2} & 0 & 0 & \frac{b}{2} & 0 & 0 & -\frac{b}{2} & 0 & 0 & \frac{b}{2} & 0 \\
\frac{b^2}{12a} & 0 & -\frac{b}{2a} & -\frac{b^2}{12a} & \frac{b}{2} & \frac{b}{2a} & -\frac{b^2}{12a} & 0 & -\frac{b}{2a} & \frac{b^2}{12a} & \frac{b}{2} & \frac{b}{2a} \\
0 & -\frac{b}{6} & 0 & 0 & \frac{b}{6} & 0 & 0 & -\frac{b}{3} & 0 & 0 & \frac{b}{3} & 0 \\
0 & 0 & 0 & 0 & \frac{b}{2} & 0 & 0 & \frac{b}{6} & -\frac{b}{a} & 0 & \frac{b}{3} & \frac{b}{a} \\
\frac{b^2}{30a} & 0 & -\frac{3b}{20a} & -\frac{b^2}{30a} & \frac{b}{6} & \frac{3b}{20a} & -\frac{b^2}{20a} & 0 & -\frac{7b}{20a} & \frac{b^2}{20a} & \frac{b}{3} & \frac{7b}{20a} \\
0 & -\frac{b}{12} & 0 & 0 & \frac{b}{12} & 0 & 0 & -\frac{b}{4} & 0 & 0 & \frac{b}{4} & 0 \\
-\frac{a}{2} & 0 & 0 & -\frac{a}{2} & 0 & 0 & \frac{a}{2} & 0 & 0 & \frac{a}{2} & 0 & 0 \\
-\frac{a}{6} & 0 & 0 & -\frac{a}{3} & 0 & 0 & \frac{a}{6} & 0 & 0 & \frac{a}{3} & 0 & 0 \\
0 & \frac{a^2}{12b} & -\frac{a}{2b} & 0 & -\frac{a^2}{12b} & -\frac{a}{2b} & \frac{a}{2} & -\frac{a^2}{12b} & \frac{a}{2b} & \frac{a}{2} & \frac{a^2}{12b} & \frac{a}{2b} \\
-\frac{a}{12} & 0 & 0 & -\frac{a}{4} & 0 & 0 & \frac{a}{12} & 0 & 0 & \frac{a}{4} & 0 & 0 \\
0 & \frac{a^2}{30b} & -\frac{3a}{20b} & 0 & -\frac{a^2}{20b} & -\frac{7a}{20b} & \frac{a}{6} & -\frac{a^2}{30b} & \frac{3a}{20b} & \frac{a}{3} & \frac{a^2}{20b} & \frac{7a}{20b} \\
0 & 0 & 0 & \frac{a}{6} & 0 & -\frac{a}{b} & \frac{a}{2} & 0 & 0 & \frac{a}{3} & 0 & \frac{a}{b} \\
0 & 0 & -2 & 0 & 0 & 2 & 0 & 0 & 2 & 0 & 0 & -2 \\
0 & \frac{a}{6} & -1 & 0 & -\frac{a}{6} & 1 & 0 & -\frac{a}{6} & 1 & 0 & \frac{a}{6} & -1 \\
\frac{b}{6} & 0 & -1 & -\frac{b}{6} & 0 & 1 & -\frac{b}{6} & 0 & 1 & \frac{b}{6} & 0 & -1 \\
0 & \frac{2a}{15} & -\frac{3}{5} & 0 & -\frac{a}{5} & \frac{3}{5} & 0 & -\frac{2a}{15} & \frac{3}{5} & 0 & \frac{a}{5} & -\frac{3}{5} \\
\frac{2b}{15} & 0 & -\frac{3}{5} & -\frac{2b}{15} & 0 & \frac{3}{5} & -\frac{b}{5} & 0 & \frac{3}{5} & \frac{b}{5} & 0 & -\frac{3}{5} \\
0 & 0 & 0 & 0 & \frac{b}{2} & 0 & 0 & \frac{b}{5} & -\frac{9b}{10a} & 0 & \frac{b}{5} & \frac{9b}{10a} \\
0 & 0 & 0 & 0 & \frac{b}{6} & 0 & 0 & \frac{b}{12} & -\frac{b}{2a} & 0 & \frac{b}{4} & \frac{b}{2a} \\
\frac{b^2}{60a} & 0 & -\frac{b^2}{15a} & -\frac{b^2}{60a} & \frac{b}{12} & \frac{b}{15a} & -\frac{b^2}{30a} & 0 & -\frac{4b}{15a} & \frac{b^2}{30a} & \frac{b}{4} & \frac{4b}{15a} \\
0 & -\frac{b}{20} & 0 & 0 & \frac{b}{20} & 0 & 0 & -\frac{b}{5} & 0 & 0 & \frac{b}{5} & 0 \\
-\frac{a}{20} & 0 & 0 & -\frac{a}{5} & 0 & 0 & \frac{a}{20} & 0 & 0 & \frac{a}{5} & 0 & 0 \\
0 & \frac{a^2}{60b} & -\frac{a}{15b} & 0 & -\frac{a^2}{30b} & -\frac{4a}{15b} & \frac{a}{12} & -\frac{a^2}{60b} & \frac{a}{15b} & \frac{a}{4} & \frac{a^2}{30b} & \frac{4a}{15b} \\
0 & 0 & 0 & \frac{a}{12} & 0 & -\frac{a}{2b} & \frac{a}{6} & 0 & 0 & \frac{a}{4} & 0 & \frac{a}{2b} \\
0 & 0 & 0 & \frac{a}{5} & 0 & -\frac{9a}{10b} & \frac{a}{2} & 0 & 0 & \frac{a}{5} & 0 & \frac{9a}{10b} \\
0 & \frac{a}{10} & -\frac{2}{5} & 0 & -\frac{a}{5} & \frac{2}{5} & 0 & -\frac{a}{10} & \frac{2}{5} & 0 & \frac{a}{5} & -\frac{2}{5} \\
\frac{b}{10} & 0 & -\frac{2}{5} & -\frac{b}{10} & 0 & \frac{2}{5} & -\frac{b}{5} & 0 & \frac{2}{5} & \frac{b}{5} & 0 & -\frac{2}{5}
\end{bmatrix}
$$

Figure 10. Matrix [T]

The total complementary energy is

$$U + W = \Pi = \frac{1}{2} [\beta]^T [H][\beta] - [\beta]^T [T][q] . \tag{42}$$

Since the total complementary energy is stationary, it's variation with respect to the stress coefficients β must vanish.

$$\frac{\partial \Pi}{\partial \beta} = 0 = \frac{1}{2} ([H][\beta] + [\beta]^T [H]) - [T][q]$$

or

$$[H][\beta] = [T][q] .$$

Solving for $[\beta]$,

$$[\beta] = [H]^{-1}[T][q] .$$

Substituting this value of $[\beta]$ into equation (32) yields

$$U = \frac{1}{2} [q]^T [T]^T [H]^{-1} [H][H]^{-1}[T][q]$$

and hence

$$U = \frac{1}{2} [q]^T [T]^T [H]^{-1}[T][q] . \tag{43}$$

The internal strain energy can also be expressed in terms of the corner displacements $[q]$ and the related forces, $[Q]$

$$U = \frac{1}{2} [Q]^T [q] . \tag{44}$$

Consequently, utilizing the definition of stiffness,

$$[Q] = [k][q] ,$$

one obtains

$$U = \frac{1}{2} \{q\}^T [k][q] \quad . \tag{45}$$

Comparing equations (43) and (45), the elemental stiffness is therefore found to be

$$[k_e] = [T]^T [H]^{-1} [T] \quad . \tag{46}$$

CHAPTER III

STIFFNESS MODIFYING MATRIX

3.1 Stiffness Modifying Matrix

The elemental stiffness developed in the preceding chapter will now be modified to include the effect of the in-plane loads on the stiffness.

Assuming a third order polynomial in x and y as a displacement function,

$$w = \alpha_1 + \alpha_2 x + \alpha_3 y + \alpha_4 x^2 + \alpha_5 xy + \alpha_6 y^2 + \alpha_7 x^3 + \alpha_8 x^2 y + \alpha_9 xy^2 + \alpha_{10} y^3 + \alpha_{11} x^3 y + \alpha_{12} xy^3 \ . \tag{47}$$

The potential energy due to the in-plane forces acting through the bending displacements is

$$V = \frac{1}{2} \int_S \sum_{i=1}^{n} \left[\sigma_x \left(\frac{\partial w}{\partial x}\right)^2 + \sigma_y \left(\frac{\partial w}{\partial y}\right)^2 + \tau_{xy} \frac{\partial w}{\partial x} \frac{\partial w}{\partial y} \right] t_i \ ds \ . \tag{48}$$

This can be formulated, matrix-wise, as

$$V = \frac{1}{2} \int_S \sum_{i=1}^{n} [\chi]^T [\sigma] [\chi] \ t_i \ ds \tag{49}$$

where

$$[\sigma] = \begin{bmatrix} \sigma_x & \tau_{xy} \\ \tau_{xy} & \sigma_y \end{bmatrix}$$

and

$$[\chi] = \begin{bmatrix} \frac{\partial w}{\partial x} \\ \\ \frac{\partial w}{\partial y} \end{bmatrix}$$

Evaluating the assumed displacement function of equation (47) and its derivatives results in the set of equations

$$\theta_{x_1} = -\alpha_3$$

$$\theta_{y_1} = -\alpha_2$$

$$w_1 = \alpha_1$$

$$\theta_{x_2} = -\alpha_3 - a\alpha_5 - a^2\alpha_8 - a^3\alpha_{11}$$

$$\theta_{y_2} = -\alpha_2 - 2a\alpha_4 - 3a^2\alpha_7$$

$$w_2 = \alpha_1 + a\alpha_2 + a^2\alpha_4 + a^3\alpha_7$$

$$\theta_{x_3} = -\alpha_3 - 2b\alpha_6 - 3b^2\alpha_{10}$$

$$\theta_{y_3} = -\alpha_2 - b\alpha_5 - b^2\alpha_9 - b^3\alpha_{12}$$

$$w_3 = \alpha_1 + b\alpha_3 + b^2\alpha_6 + b^3\alpha_{10}$$

$$\theta_{x_4} = -\alpha_3 - a\alpha_5 - 2b\alpha_6 - a^2\alpha_8 - 2ab\alpha_9 - 3b^2\alpha_{10} - a^3\alpha_{11} - 3ab^2\alpha_{12}$$

$$\theta_{y_4} = -\alpha_2 - 2a\alpha_4 - b\alpha_5 - 3a^2\alpha_7 - 2ab\alpha_8 - b^2\alpha_9 - 3a^2b\alpha_{11} - b^3\alpha_{12}$$

$$w_4 = \alpha_1 + a\alpha_2 + b\alpha_3 + a^2\alpha_4 + ab\alpha_5 + b^2\alpha_6 + a^3\alpha_7 + a^2b\alpha_8 + ab^2\alpha_9 + b^3\alpha_{10} + a^3b\alpha_{11} + ab^3\alpha_{12} \qquad (50)$$

Or in matrix form,

$$[q] = [A][\alpha] \tag{51}$$

where $[q]$ is, as before, the nodal displacements.

Solving (46) for $[\alpha]$

$$[\alpha] = [A]^{-1}[q] \ . \tag{52}$$

Also, $[\chi]$ can be expressed

$$[\chi] = \begin{bmatrix} \frac{\partial w}{\partial x} \\ \\ \frac{\partial w}{\partial y} \end{bmatrix} = [B][\alpha] = [B][A]^{-1}[q] \tag{53}$$

where $[B]$ is

$$\begin{bmatrix} 0 & 1 & 0 & 2x & y & 0 & 3x^2 & 2xy & y^2 & 0 & 3x^2y & y^3 \\ 0 & 0 & 1 & 0 & x & 2y & 0 & x^2 & 2xy & 3y^2 & x^3 & 3xy^2 \end{bmatrix}$$

Now inserting the expression for $[\chi]$ into equation (49) yields

$$V = \frac{1}{2} \oint_S \sum_{i=1}^{n} [q]^T[A^{-1}]^T[B]^T[\sigma][B][A^{-1}][q] \ t_i \ ds \ .$$

Again by comparing to equation (45),

$$[k_m] = \oint_S \sum_{i=1}^{n} [A^{-1}]^T[B]^T[\sigma][B][A^{-1}] \ t_i \ ds \ .$$

Since $[A]$ and hence $[A^{-1}]$ are constant matrices, they can be excluded from the integration. Therefore,

$$[k_m] = [A^{-1}]^T \left\{ \oint_S \sum_{i=1}^{n} [B]^T[\sigma]]B] \ t_i \ ds \right\} [A^{-1}] \ .$$

Let

$$\int_S \sum_{i=1}^{n} [B]^T[\sigma][B]\, t_i\, ds = [BS]. \qquad (54)$$

Then [BS] can be evaluated for any specific $[\sigma]$.

For example, σ_x, σ_y, and τ_{xy} can be taken as constants or as functions of x or y or both, representing the distribution of in-plane stresses in the element. Also, the modifying stiffnesses can be added together thereby making it possible to accomodate virtually any stress distribution in the element. This in turn means that any variation of in-plane forces may be applied, both at the edges and as surface tractions.

As an example, [BS] will be evaluated for σ_x = constant within the element and $\sigma_y = \tau_{xy} = 0$ throughout the element. This would be the case of a uniform uniaxial in-plane loading.

Since σ_x and the sum of the thickness of membrane cores are constant throughout the element, they can be removed as scalar multipliers of matrix [BS]. Matrix [BS] is shown in Figure 11.

$[k_m]$ is now determinate and can be used to modify an elemental bending stiffness thereby including the effect of the in-plane loads upon the stiffness.

3.2 In-plane Stiffness

It should now be noted that although in most cases a proper assumption can be made for the stress distribution, it is not always so. For instance, concentrated loads in the plane of the plate applied in an irregular pattern would make it difficult to be sure that the stress pattern assumed was appropriate.

For this reason the in-plane stiffness matrix is developed here after the method of Pian (13) but modified to apply to layered plates

$$\sigma \sum_{i=1}^{n} t_i \begin{bmatrix}
0 & 0 & 0 & 0 & 0 & 0 & 0 & 0 & 0 & 0 & 0 & 0 \\
 & ab & 0 & a^2b & \frac{ab^2}{2} & 0 & a^3b & \frac{a^2b^2}{2} & \frac{ab^3}{3} & 0 & \frac{a^3b^2}{2} & \frac{ab^4}{4} \\
 & & 0 & 0 & 0 & 0 & 0 & 0 & 0 & 0 & 0 & 0 \\
 & & & \frac{4a^3b}{3} & \frac{a^2b^2}{2} & 0 & \frac{3a^4b}{2} & \frac{2a^3b^2}{3} & \frac{a^2b^3}{3} & 0 & \frac{3a^4b^2}{4} & \frac{a^2b^4}{4} \\
 & & & & \frac{ab^3}{3} & 0 & \frac{a^3b^2}{2} & \frac{a^2b^3}{3} & \frac{ab^4}{4} & 0 & \frac{a^3b^3}{3} & \frac{ab^5}{5} \\
 & & & & & 0 & 0 & 0 & 0 & 0 & 0 & 0 \\
 & & & & & & \frac{9a^5b}{5} & \frac{3a^4b^2}{4} & \frac{a^3b^3}{3} & 0 & \frac{9a^5b^3}{10} & \frac{a^3b^4}{4} \\
 & & & & & & & \frac{4a^3b^3}{9} & \frac{a^2b^4}{4} & 0 & \frac{a^4b^3}{2} & \frac{a^2b^5}{5} \\
 & & \text{SYMMETRICAL} & & & & & & \frac{ab^5}{5} & 0 & \frac{a^3b^4}{4} & \frac{ab^6}{6} \\
 & & & & & & & & & 0 & 0 & 0 \\
 & & & & & & & & & & \frac{3a^5b^3}{5} & \frac{a^3b^5}{5} \\
 & & & & & & & & & & & \frac{ab^7}{7}
\end{bmatrix}$$

Figure 11. Matrix [BS]

and including all second order terms in the stress function since the application of the results will be to describe the stress pattern as closely as possible.

The strain energy U_p due to the deformation of the middle plane of the plate by in-plane forces is

$$U_p = \frac{1}{2} \int_V [\sigma_x \epsilon_x + \sigma_y \epsilon_y + \tau_{xy} \gamma_{xy}] \, dv \, . \tag{55}$$

Since only small deflections are to be acknowledged, then σ_x, σ_y, and τ_{xy} may be considered to remain unchanged during bending.

The preceding statement of U_p can be expressed in matrix form as

$$U_p = \frac{1}{2} \int_V [\sigma_p][\epsilon] \, dv = \frac{1}{2} \int_V [\sigma_p][N_p][\sigma_p] \, dv \tag{56}$$

where

$$[\sigma_p] = \begin{bmatrix} \sigma_x \\ \sigma_y \\ \tau_{xy} \end{bmatrix}$$

and $[N_p]$ is the upper left 3×3 matrix portion of $[N]$ as defined in Chapter II.

Proceeding as in Chapter II this leads to an equation similar to (33)

$$[H_p] = \int_A \sum_T [P_p][N][P_p] \, t_{i,j} \, dA \tag{57}$$

where

$$[\sigma_p] = [P_p][\rho] \, . \tag{58}$$

The assumed stress functions are

$$\sigma_x = \rho_1 + \rho_2\bar{x} + \rho_3\bar{y} + \rho_4\bar{x}^2 + \rho_5\bar{x}\bar{y} + \rho_6\bar{y}^2 \tag{59}$$

$$\sigma_y = \rho_7 + \rho_8\bar{x} + \rho_9\bar{y} + \rho_{10}\bar{x}^2 + \rho_{11}\bar{x}\bar{y} + \rho_{12}\bar{y}^2 \tag{60}$$

$$\tau_{xy} = \rho_{13} + \rho_{14}\bar{x} + \rho_{15}\bar{y} + \rho_{16}\bar{x}^2 + \rho_{17}\bar{x}\bar{y} + \rho_{18}\bar{y}^2 \ . \tag{61}$$

From the equilibrium of the in-plane forces on the elements,

$$\frac{\partial\sigma_x}{\partial x} + \frac{\partial\tau_{xy}}{\partial y} = 0 \tag{62}$$

$$\frac{\partial\tau_{xy}}{\partial x} + \frac{\partial\sigma_y}{\partial y} = 0 \ . \tag{63}$$

Taking the appropriate partial derivatives, six of the eighteen coefficients assumed in the stress functions can be eliminated, resulting in the following equilibriated stress functions

$$\sigma_x = \rho_1 + \rho_2\bar{x} + \rho_3\bar{y} + \rho_4\bar{x}^2 + \rho_5\bar{x}\bar{y} + \rho_6\bar{y}^2 \tag{64}$$

$$\sigma_y = \frac{b^2\bar{y}^2}{a^2}\rho_4 + \rho_7 + \rho_8\bar{x} + \rho_9\bar{y} + \rho_{10}\bar{x}^2 + \rho_{11}\bar{x}\bar{y} \tag{65}$$

$$\tau_{xy} = -\frac{b\bar{y}}{a}\rho_2 - \frac{2b\bar{x}\bar{y}}{a}\rho_4 - \frac{b\bar{y}^2}{2a}\rho_5 - \frac{a\bar{x}}{b}\rho_9 - \frac{a\bar{x}^2}{2b}\rho_{11} + \rho_{13} \ . \tag{66}$$

From this formulation the matrix $[P_p]$ of equation (58) can be written and $[H_p]$ is then determinate from equation (57). Performing the appropriate integrations and summations, $[H_p]$ can now be evaluated and is shown in Figure 12.

Following the procedure that was outlined in Chapter II,

$$[T_p] = \oint [R_p]^T [L_p] \, ds \tag{67}$$

where the relationships

$$
\begin{bmatrix}
A & \frac{A}{2} & \frac{A}{2} & \frac{A}{3}-\frac{Wab^2}{3a^2} & \frac{A}{4} & \frac{A}{3} & -WA & -\frac{WA}{2} & -\frac{WA}{2} & -\frac{WA}{3} & -\frac{WA}{4} & 0 \\
 & \frac{A}{3}+\frac{Vb^2}{3a^2} & \frac{A}{4} & \frac{A}{4}-\frac{WAb^2}{6a^2}+\frac{Wab^2}{3a^2} & \frac{A}{6}+\frac{VAb^2}{8a^2} & \frac{A}{6} & -\frac{WA}{2} & -\frac{WA}{3} & -\frac{WAb}{4}+\frac{VA}{4} & -\frac{WA}{4} & -\frac{WA}{6}+\frac{VA}{12} & -\frac{VAb}{2a} \\
 & & \frac{A}{3} & \frac{A}{6}-\frac{WAb^2}{4a^2} & \frac{A}{6} & \frac{A}{4} & -\frac{WA}{2} & -\frac{WA}{4} & -\frac{WA}{3} & -\frac{WA}{6} & -\frac{WA}{6} & 0 \\
 & & & \frac{A}{5}-\frac{2WAb^2}{9a^2}+\frac{Ab^4}{5a^4}+\frac{4VAb^2}{9a^2} & \frac{A}{8}-\frac{WAb^2}{a^2}+\frac{VAb^2}{8a^2} & \frac{A}{9}-\frac{WAb^2}{5a^2} & -\frac{WA}{3}+\frac{Ab^2}{3a^2} & -\frac{WA}{4}+\frac{Ab^2}{6a^2} & -\frac{WA}{6}+\frac{Ab^2}{4a^2}+\frac{VA}{3} & -\frac{WA}{5}+\frac{Ab^2}{9a^2} & -\frac{WA}{8}+\frac{Ab^2}{8a^2}+\frac{VA}{8} & -\frac{VAb}{2a} \\
 & & & & \frac{A}{9}+\frac{VAb^2}{20a^2} & \frac{A}{8} & -\frac{WA}{4} & -\frac{WA}{6} & -\frac{WA}{6}+\frac{VA}{12} & -\frac{WA}{8} & -\frac{WA}{9}+\frac{VA}{36} & -\frac{VAb}{6a} \\
 & & & & & \frac{A}{5} & -\frac{WA}{3} & -\frac{WA}{6} & -\frac{WA}{4} & -\frac{WA}{9} & -\frac{WA}{8} & 0 \\
 & \multicolumn{11}{l}{S\ Y\ M\ M\ E\ T\ R\ I\ C} \\
 & & & & & & A & \frac{A}{2} & \frac{A}{2} & \frac{A}{3} & \frac{A}{4} & 0 \\
 & \multicolumn{11}{l}{A = \frac{ab}{E}\sum_{i=1}^{n} t_i} \\
 & & & & & & & \frac{A}{3} & \frac{A}{4} & \frac{A}{4} & \frac{A}{6} & 0 \\
 & \multicolumn{11}{l}{W = \upsilon} \\
 & & & & & & & & \frac{A}{3}+\frac{VAa^2}{3b^2} & \frac{A}{6} & \frac{A}{6}+\frac{VAa^2}{8b^2} & -\frac{VAa}{2b} \\
 & \multicolumn{11}{l}{V = \bar{\upsilon}} \\
 & & & & & & & & & \frac{A}{5} & \frac{A}{8} & 0 \\
 & & & & & & & & & & \frac{A}{9}+\frac{VAa^2}{20b^2} & -\frac{VAa}{6b} \\
 & & & & & & & & & & & VA
\end{bmatrix}
$$

Figure 12. Matrix $[H_p]$

$$[\varepsilon_p] = [R_p][\rho] \tag{68}$$

$$[u_p] = [L_p][q_p] \tag{69}$$

are used, and noting

$$[S_p] = \begin{bmatrix} S_{x_{12}} \\ S_{y_{12}} \\ S_{x_{24}} \\ S_{y_{24}} \\ S_{x_{34}} \\ S_{y_{34}} \\ S_{x_{13}} \\ S_{y_{13}} \end{bmatrix} = \sum_{i=1}^{n} t_i \begin{bmatrix} -\tau_{12} \\ -\sigma_{12} \\ \sigma_{24} \\ \tau_{24} \\ \tau_{34} \\ \sigma_{34} \\ -\sigma_{13} \\ -\tau_{13} \end{bmatrix}$$

$[R_p]$ may be calculated and is shown in Figure 13.

If $\bar{u}$ is defined as displacement in the x-direction and $\bar{v}$ as displacement in the y-direction,

$$[u_p] = \begin{bmatrix} \bar{u}_{12} \\ \bar{v}_{12} \\ \bar{u}_{24} \\ \bar{v}_{24} \\ \bar{u}_{34} \\ \bar{v}_{34} \\ \bar{u}_{13} \\ \bar{v}_{13} \end{bmatrix}, \qquad [q] = \begin{bmatrix} \bar{u}_1 \\ \bar{v}_1 \\ \bar{u}_2 \\ \bar{v}_2 \\ \bar{u}_3 \\ \bar{v}_3 \\ \bar{u}_4 \\ \bar{v}_4 \end{bmatrix}$$

$$\sum_{i=1}^{n} t_i \begin{bmatrix}
0 & 0 & 0 & 0 & 0 & 0 & 0 & 0 & \frac{a\bar{x}}{b} & 0 & \frac{a\bar{x}^2}{2b} & -1 \\
0 & 0 & 0 & 0 & 0 & 0 & -1 & -\bar{x} & 0 & -\bar{x}^2 & 0 & 0 \\
1 & 1 & \bar{y} & 1 & \bar{y} & \bar{y}^2 & 0 & 0 & 0 & 0 & 0 & 0 \\
0 & -\frac{b\bar{y}}{a} & 0 & -\frac{2b\bar{y}}{a} & -\frac{b\bar{y}^2}{2a} & 0 & 0 & 0 & -\frac{a}{b} & 0 & -\frac{a}{2b} & 1 \\
0 & -\frac{b}{a} & 0 & -\frac{2b\bar{x}}{a} & -\frac{b}{2a} & 0 & 0 & 0 & -\frac{a\bar{x}}{b} & 0 & -\frac{a\bar{x}^2}{2b} & 1 \\
0 & 0 & 0 & \frac{b^2}{a^2} & 0 & 0 & 1 & \bar{x} & 1 & \bar{x}^2 & \bar{x} & 0 \\
-1 & 0 & -\bar{y} & 0 & 0 & -\bar{y}^2 & 0 & 0 & 0 & 0 & 0 & 0 \\
0 & \frac{b\bar{y}}{a} & 0 & 0 & \frac{b\bar{y}^2}{2a} & 0 & 0 & 0 & 0 & 0 & 0 & -1
\end{bmatrix}$$

Figure 13. Matrix $[R_p]$

Then, from equation (69) $[L_p]$ may be formed.

$$\begin{bmatrix}
1-\bar{x} & 0 & \bar{x} & 0 & 0 & 0 & 0 & 0 \\
0 & 1-\bar{x} & 0 & \bar{x} & 0 & 0 & 0 & 0 \\
0 & 0 & 1-\bar{y} & 0 & 0 & 0 & \bar{y} & 0 \\
0 & 0 & 0 & 1-\bar{y} & 0 & 0 & 0 & \bar{y} \\
0 & 0 & 0 & 0 & 1-\bar{x} & 0 & \bar{x} & 0 \\
0 & 0 & 0 & 0 & 0 & 1-\bar{x} & 0 & \bar{x} \\
1-\bar{y} & 0 & 0 & 0 & \bar{y} & 0 & 0 & 0 \\
0 & 1-\bar{y} & 0 & 0 & 0 & \bar{y} & 0 & 0
\end{bmatrix}$$

Performing the manipulations indicated in (67), $[T_p]$ can now be determined and is shown in Figure 14.

Consequently, adding the p subscripts to equation (46) yields

$$[k_p] = [T_p]^T [H_p^{-1}][T_p] \tag{70}$$

and the in-plane stiffness of the element can be computed.

$$\sum_{i=1}^{n} t_i \begin{bmatrix}
-\frac{b}{2} & 0 & \frac{b}{2} & 0 & -\frac{b}{2} & 0 & \frac{b}{2} & 0 \\
0 & \frac{b^2}{6a} & \frac{b}{2} & -\frac{b^2}{6a} & -\frac{b}{2} & \frac{b^2}{3a} & 0 & -\frac{b^2}{3a} \\
-\frac{b}{6} & 0 & \frac{b}{6} & 0 & -\frac{b}{3} & 0 & \frac{b}{3} & 0 \\
0 & 0 & \frac{b}{2} & -\frac{b^2}{3a} & -\frac{b}{3} & \frac{b^2}{2a} & -\frac{b}{6} & -\frac{b^2}{6a} \\
0 & \frac{b^2}{24a} & \frac{b}{6} & -\frac{b^2}{24a} & -\frac{b}{4} & \frac{b^2}{8a} & \frac{b}{12} & -\frac{b^2}{8a} \\
-\frac{b}{12} & 0 & \frac{b}{12} & 0 & -\frac{b}{4} & 0 & \frac{b}{4} & 0 \\
0 & -\frac{a}{2} & 0 & -\frac{a}{2} & 0 & \frac{a}{2} & 0 & \frac{a}{2} \\
0 & -\frac{a}{6} & 0 & -\frac{a}{3} & 0 & \frac{a}{6} & 0 & \frac{a}{3} \\
\frac{a^2}{6b} & 0 & \frac{a^2}{3b} & -\frac{a}{2} & -\frac{a^2}{6b} & \frac{a}{2} & -\frac{a^2}{3b} & 0 \\
0 & -\frac{a}{12} & 0 & -\frac{a}{4} & 0 & \frac{a}{12} & 0 & \frac{a}{4} \\
\frac{a^2}{24b} & 0 & \frac{a^2}{8b} & -\frac{a}{4} & -\frac{a^2}{24b} & \frac{a}{6} & -\frac{a^2}{8b} & \frac{a}{12} \\
-\frac{a}{2} & -\frac{b}{2} & -\frac{a}{2} & \frac{b}{2} & \frac{a}{2} & -\frac{b}{2} & \frac{a}{2} & \frac{b}{2}
\end{bmatrix}$$

Figure 14. Matrix $[T_p]$

CHAPTER IV

COMPUTATION OF PLATE DEFLECTIONS

4.1 Assembly of Elements

In the previous sections, the necessary steps for the computation of the elemental stiffnesses of multilayer plates in bending including consideration of the effect of in-plane loads have been developed. They can now be assembled to provide the stiffness of the entire plate.

The stiffness of the entire plate is formed by constructing a new stiffness matrix whose dimensions are equal to the total number of degrees of freedom for the entire plate. Each term of the matrix is found by adding the corresponding values of the elemental stiffnesses for each degree of freedom.

For example, a 4×4 grid would result in 25 nodes. Since each node is considered to have three degrees of freedom, this would require a 75×75 matrix. It is in handling support conditions that this method demonstrates its greatest justification compared to the more classical procedures.

Any of the generalized coordinate or generalized forces can be specified. This provides for most of the physically possible conditions. Some examples of boundary condition applications are as follows.

(a) For a simply supported edge, the deflection at the node and either the tangential slope or the edge twisting moment may

be taken as zero.

(b) Clamped edge - all three generalized coordinates are taken to be zero.

(c) Column support - deflection only is set equal to zero.

The stiffness matrix is now reordered according to the following procedure. Designating

zero generalized coordinates = q_o,

specified non-zero generalized coordinates = q_n,

unknown generalized forces = q_u,

zero generalized forces = Q_o,

specified non-zero generalized forces = Q_n,

unknown generalized forces = Q_u,

the stiffness relationship can be partitioned and written as

$$\begin{bmatrix} Q_o \\ Q_n \\ Q_{u_1} \\ Q_{u_2} \end{bmatrix} = \begin{bmatrix} K_{11} & K_{12} & K_{13} & K_{14} \\ K_{21} & K_{22} & K_{23} & K_{24} \\ K_{31} & K_{32} & K_{33} & K_{34} \\ K_{41} & K_{42} & K_{43} & K_{44} \end{bmatrix} \begin{bmatrix} q_{u_1} \\ q_{u_2} \\ q_n \\ q_o \end{bmatrix} \tag{71}$$

Multiplying out the first line,

$$Q_o = K_{11}q_{u_1} + K_{12}q_{u_2} + K_{13}q_n + K_{14}q_o .$$

Noting that K_{11}, K_{12}, K_{13}, K_{14}, q_n, q_o, and Q_o are known, and specifically that q_o is zero,

$$Q_o = K_{11}q_{u_1} + K_{12}q_{u_2} + K_{13}q_n . \tag{72}$$

From the second line of (63),

$$Q_n = K_{21}q_{u_1} + K_{22}q_{u_2} + K_{23}q_n + K_{24}q_o \ .$$

However, again $Q_o = 0$, therefore,

$$Q_n = K_{21}q_{u_1} + K_{22}q_{u_2} + K_{23}q_n \ . \tag{73}$$

Solving this expression for q_{u_2},

$$q_{u_2} = K_{22}^{-1}(Q_n - K_{21}q_{u_1} - K_{23}q_n) \ . \tag{74}$$

Substituting into equation (72),

$$q_{u_1} = (K_{12}K_{22}K_{21} - K_{11})^{-1}(K_{12}K_{22}^{-1}Q_n - K_{23}q_n - Q_o) \ , \tag{75}$$

where all the terms on the right side are specified, thus making it possible to solve for q_{u_1}. Substituting these values back into equation (74) provides a solution for the remainder of the unknown generalized coordinates, q_{u_2}.

If all of the specified generalized coordinates are of zero value, a simpler procedure is possible. Letting Q_o now represent any specified generalized forces, the partitioning now results in

$$\begin{bmatrix} Q_o \\ Q_u \end{bmatrix} = \begin{bmatrix} K_{11} & K_{12} \\ K_{21} & K_{22} \end{bmatrix} \begin{bmatrix} q_u \\ q_o \end{bmatrix} \tag{76}$$

and, from the first line,

$$Q_o = K_{11}q_u + K_{12}q_o \ .$$

But since $q_o = 0$,

$$Q_o = K_{11}q_u$$

or

$$q_u = K_{11}^{-1} Q_o \quad . \tag{77}$$

The unknown generalized coordinates may now be solved for directly.

Loads corresponding to the generalized coordinates (M_y, M_x, Q_z) may be applied at any node where the generalized displacement has been designated as unknown.

In the partitioning of equation (71) these would be the forces denoted Q_n. In the simpler formulation of equation (76) they could be any of those in the submatrix Q_o.

4.2 Loads

Loads in the plane of the plate can be accommodated by combining the bending stiffness matrix developed in Chapter II with the bending stiffness modifier developed in Section 3.1 and the in-plane stiffness matrix developed in Section 3.2. This results in five degrees of freedom at each node, and loads can be applied both at the nodes and as stresses. If the in-plane stiffness matrix of Section 3.2 is not considered, the number of degrees of freedom per node can be reduced to three. This a substantial savings in computer storage, while neglecting a relatively minor effect. This reduced form has been used in this thesis. The loads are then applied as stresses.

CHAPTER V

CRITICAL STRESS SOLUTION

5.1 General

Once the total stiffness matrix of the layered plate has been established, a characteristic equation form can be obtained. A solution procedure has been presented in papers by Hartz (17) and by Kapur and Hartz (18) and has been credited to Bolotin (19). Essentially the same method is used by Gallagher and Padlog (20) and by Archer (21) with some variations. Some complications arise because the stiffness matrix yields the highest mode first in an iterative solution. Since interest is usually centered around the lower modes, it may be desirable to change the form to a flexibility type providing the lower modes first. The preceding method will yield the critical stresses utilizing the foregoing stiffness matrices and is particularly appropriate if all of the modes are required.

Another approach will be investigated here. It tends to be very efficient for determination of the critical stress corresponding to the fundamental mode and fairly good for other low order modes. It also has the advantage of being physical in nature and provides some opportunity to study the behavior during unbounded deflection. The method consists of predicting the critical load by using a fast converging prediction-correction method.

5.2 Magnification Factor

Timoshenko (18) shows that the following differential equation governs a plate that is subjected to: an initial deflection w_o; an additional deflection w_1 caused by the transverse loads; and in-plane loads N_x, N_y, and N_{xy}.

$$\frac{\partial^4 w_1}{\partial x^4} + 2\frac{\partial^4 w_1}{\partial x^2 \partial y^2} + \frac{\partial^4 w_1}{\partial y^4} = \frac{1}{D}\left[q + N_x \frac{\partial^2 (w_o + w_1)}{\partial x^2} + N_y \frac{\partial^2 (w_o + w_1)}{\partial y^2} + 2N_{xy} \frac{\partial^2 (w_o + w_1)}{\partial x \partial y}\right].$$

For multilayer plates the equation will be similar and is approximated by

$$\frac{\partial^4 w_1}{\partial x^4} + 2\frac{\partial^4 w_1}{\partial x^2 \partial y^2} + \frac{\partial^4 w_1}{\partial y^4} = \frac{1}{D}\sum_{i=1}^{n} t_i \left[q + \sigma_x \frac{\partial^2 (w_o + w_1)}{\partial x^2} + \sigma_y \frac{\partial^2 (w_o + w_1)}{\partial y^2} + 2\tau_{xy} \frac{\partial^2 (w_o + w_1)}{\partial x \partial y}\right] \quad (78)$$

If the initial deflection surface, represented by

$$w_o = \sum_{m=1}^{\infty} \sum_{n=1}^{\infty} a_{mn} \sin \frac{m\pi x}{a} \sin \frac{n\pi y}{b} \quad (79)$$

is substituted into equation (78) the expression for additional deflections of a uniaxially loaded, simply supported plate is found to be

$$w_1 = \sum_{m=1}^{\infty} \sum_{n=1}^{\infty} \frac{a_{mn}\sigma_x}{\frac{\pi^2 \bar{D}}{a^2}\left(m + \frac{n^2 a^2}{mb^2}\right)^2 - \sigma_x} \sin \frac{m\pi x}{a} \sin \frac{n\pi y}{b}$$

in which

$$\bar{D} = \frac{D}{\sum_{i=1}^{n} t_i} .$$

The total deflection is

$$w = w_0 + w_1 = \sum_{m=1}^{\infty} \sum_{n=1}^{\infty} \frac{a_{mn}}{1 - \frac{\sigma_x}{\frac{\pi^2 \bar{D}}{a^2}\left(m + \frac{n^2 a^2}{mb^2}\right)^2}} \sin \frac{m\pi x}{a} \sin \frac{n\pi y}{b} \qquad (80)$$

Hence as σ_x approaches its critical value

$$\frac{\pi^2 \bar{D}}{a^2}\left(m + \frac{n^2 a^2}{mb^2}\right)^2 ,$$

w becomes very large.

For a simply supported rectangular plate, assuming

$$w_0 = a_{11} \sin \frac{\pi x}{a} \sin \frac{\pi y}{b} ,$$

the total deflection becomes

$$w = \frac{a_{11}}{1 - \alpha} \sin \frac{\pi x}{a} \sin \frac{\pi y}{b}$$

where

$$\alpha = \frac{\sigma_x}{\frac{\pi^2 \bar{D}}{a^2}\left(1 + \frac{a^2}{b^2}\right)^2} .$$

For maximum deflection at $x = \frac{a}{2}$, $y = \frac{b}{2}$,

$$w_{max} = \frac{a_{11}}{1 - \alpha} .$$

Noting that

$$(\sigma_x)_{critical} = \frac{\pi^2 \bar{D}}{a^2} \left(1 + \frac{a^2}{b^2}\right)^2,$$

then α can also be taken as

$$\frac{\sigma_x}{(\sigma_x)_{critical}} .$$

This then is a corollary to Southwell's development for columns (22).

Therefore, if a_{11} is an initial displacement pattern similar to the buckled configuration sought, then

$$w = \frac{w_o}{1 - \alpha}$$

or

$$(\sigma)_{critical} = \sigma \left(\frac{w}{w - w_o}\right) . \qquad (81)$$

This development is based upon the deformations conforming to a double sine series. It will be shown, however, that good results can be achieved for some plates for which the displacement configuration is not very well represented by the assumed series.

5.3 Application of Magnification Factor

The solution used herein proceeds as follows:

(a) deflection is computed due to a transverse load;

(b) a token in-plane load is applied and the deflection due to the combined loading is computed;

(c) the critical load is predicted using equation (81);

(d) the applied in-plane load and the resulting predicted critical load are compared. If the ratio of the former to the latter is less than some predetermined value (.995 for the problems in Chapter VII) then the predicted critical stress is used as the initial stress and a new critical stress computed. The two stresses are again compared and the procedure is repeated until the prescribed ratio is satisfied.

5.4 Mode Determination

If a single concentrated load or a uniformly distributed load is applied to the given plate, then the critical load will be for the most basic mode consistent with the constraints.

For example, a simply supported plate transversely loaded with a uniform load will yield the configuration conforming to the first buckling mode and hence the corresponding buckling load. The second mode can be found by considering the plate to be anti-symmetrically deformed. This can be accomplished by taking one-half of the plate and applying the constraints required to properly form the buckled mode.

Succeedingly higher modes can be found in the same manner as long as the dimensions of the segments are known. Unfortunately, the dimensions can be accurately predicted for only a few configurations. Therefore another means is required to determine higher modes.

One possible method would be to estimate the division of the plate into modes, determine the critical load of each segment, redimension the segments, and continue until the buckling load of each segment is the same. This has some obvious disadvantages. The method

that will be used here is to initially deform the plate into approximately the desired buckling mode by selective application of the transverse loads. Application of the in-plane loads will then force the plate into the mode sought and the solution will yield the critical load for that mode. This provides a relatively simple solution for the first few modes. As mentioned in Section 5.1, the eigenvalue solution is most appropriate when all the modes or some of the higher modes are required.

The displacement used in equation (74) may be any of the deflections or rotations representing the degrees of freedom of the plate. For the examples in Chapter VI the anticipated point of maximum deflection is used.

5.5 Convergence

The convergence of the method appears to be excellent. Although a relatively few problems have been solved, it does appear as though the convergence may be influenced by the selection of some arbitrary parameters involved in the solution. In extreme cases the accuracy may also be affected.

In a few cases the first prediction was within one-half of one per cent of the ultimate answer. For almost all examples two or three iterations sufficed for first mode determinations. Second and third mode solutions required more iterations, although too few problems were worked to formulate decisive conclusions. The maximum number of iterations encountered was six.

Two initial conditions that appear to effect the solution are:

(1) proximity of the initial deflected shape of the plate

(due to transverse loads only) to the buckled mode. This is discussed in the Conclusions.

(2) Selection of a degree of freedom as the displacement to be compared in equation (81). Scattered results indicate that deflections give better accuracy than rotations.

CHAPTER VI

EXAMPLES

6.1 Procedure

The method as described in the preceding chapters has been programmed on the International Business Machine 7040 electronic digital computer.

The program is divided into two segments. The first segment develops the elemental stiffnesses. The second segment combines the elemental stiffnesses into a structural stiffness matrix and solves for deflections and critical load.

The basic grid used in the following examples is four by four. If the plate is symmetric with respect to both the x and y axes, then a quarter of the plate is actually used and the effective grid is eight by eight. If there is symmetry with respect to only one axis, then the grid is four by eight. If no symmetry exists, then the actual as well as effective grid is four by four. The grid can, of course, be varied depending primarily on available computer storage.

Four sets of boundary conditions are examined in the examples. They are

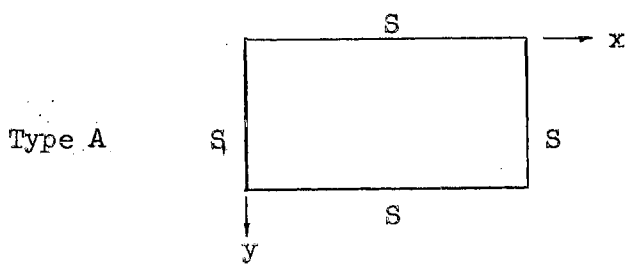

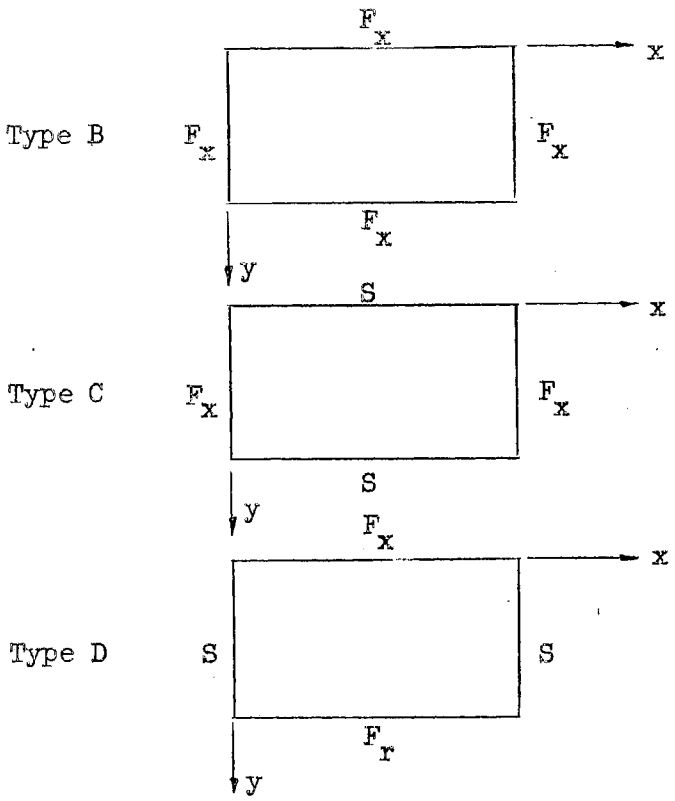

where

S = simple support

Fx = fixed support

Fr = free edge.

6.2 Homogeneous Plates

This group of problems is a control on the accuracy of the method. Results are compared with those of reference (25).

The plate used here has the following dimensions and properties:

Ly is the dimension of the plate in the y-direction and is taken equal to 100".

Lx is the dimension of the plate in the x-direction and is defined by the aspect ratio.

$E = 30 \times 10^6$ psi.

$G = \frac{E}{2(1 + \nu)} = 11.5 \times 10^6$ psi.

$\nu = .3$

t = plate thickness = 2.0".

In Table I only the critical modes are tabulated. Unless otherwise noted the critical mode is the primary mode. The loading is a uniformly distributed stress in the x-direction. For some low aspect cases the comparative results have been omitted because they did not fall within the range of Gerard's solution. Adding a uniformly distributed stress in the y-direction equal to one-half of the x-direction stress yields the results shown in Table II. Several uniaxial problems were solved for more than one mode. These are tabulated in Table III.

6.3 Sandwich Plates

Although the method developed in previous chapters is valid for multilayered plates, the illustrative examples used in this section assume a three layered plate composed of a core sandwiched between two aluminum facing layers. The group of examples solved here also serves to substantiate the method although it includes some cases for which existing solutions were not found in the literature. The plate dimensions and properties are as follows:

Ly = 23.5"

Lx is defined by the aspect ratio

TABLE I

CRITICAL STRESSES FOR HOMOGENEOUS PLATES UNIAXIALLY LOADED IN THE X-DIRECTION

Aspect Ratio	Boundary Conditions	Finite Element Solution	Existing Solution (25)
.5	A	66033	67717
.5	B	203934	
.5	C	190903	
.5	D	48050	
.75	A	46925	47652
.75	B	123945	
.75	C	104000	105000
.75	D	25862	27085
1.00	A	42743	43338
1.00	B	110034	111590
1.00	C	74687	73590
1.00	D	17751	17334
2.00	A*	45930	43338
2.00	B**	85428	86130
2.00	C*	59368	52550
2.00	D	14353	14084

* Second mode critical

** Third mode critical

TABLE II

CRITICAL STRESSES FOR BIAXIALLY
LOADED HOMOGENEOUS PLATES

Aspect Ratio	Boundary Conditions	Finite Element Solution	Existing Solution (25)
.5	A	58694	60670
.5	B	183380	188511
.5	C	174497	186000
.5	D	45915	
.75	A	35826	36800
.75	B	98846	102000
.75	C	83211	90000
1.00	A	28494	28893
1.00	B	75191	76367
1.00	C	64343	53700
2.00	A	22156	22534
2.00	B	68447	61735
2.00	C	26484	26400

TABLE III

CRITICAL STRESSES FOR VARIOUS MODES OF UNIAXIALLY LOADED HOMOGENEOUS PLATES

Aspect Ratio	Boundary Conditions	Mode	Buckling Load
2.0	A	1	66468
2.0	A	2	45930
2.0	B	1	110034
2.0	B	2	102424
2.0	B	3	85428
2.0	C	1	112661
2.0	C	2	60001
2.0	C	3	59368

two aluminum facing membrane layers

thickness = .021"

$E = 9.5 \times 10^6$ psi.

$\nu = .25$

balsa core layer

thickness = .181"

G = 19000 psi.

As before, only the critical load is shown in Table IV for a uniformly distributed stress applied in the x-direction.

The same sandwich plate is loaded biaxially with a uniformly distributed stress in the y-direction equal to one-half the x-direction stress resulting in the critical loads shown in the Table V.

A uniaxially loaded square sandwich plate example used by Hoff (4) was also checked. Hoff obtained a critical stress of 7220 psi. while the method presented here yielded 7483 as the critical stress.

6.4 Multilayer Plates

A series of related problems are solved and the results are plotted to demonstrate the application of the method to the determination of critical stress for multilayer plates.

TABLE IV

CRITICAL STRESSES FOR THREE LAYERED SANDWICH PLATES
UNIAXIALLY LOADED IN THE X-DIRECTION

Aspect Ratio	Boundary Conditions	Finite Element Solution	Existing Solution (5)
.5	A	11420	10077
.5	B	32209	
.5	C	30405	
.7	A	8076	7930
.7	B	21018	19074
.7	C	17879	15704
.7	D	9722	
1.0	A	7268	7091
1.0	B	17194	16235
1.0	C	11887	11012
2.0	A*	7268	7091
2.0	B**	13016	12786
2.0	C*	9442	8397

* Second mode critical

** Third mode critical

TABLE V

CRITICAL STRESSES FOR THREE LAYERED BIAXIALLY LOADED SANDWICH PLATES

Aspect Ratio	Boundary Conditions	Finite Element Solution	Existing Solution (26)
.5	A	10274	
.5	B	29253	
.5	C	28600	
.7	A	6487	
.7	B	17265	
.7	C	15075	
.7	D	6927	
1.0	A	4834	4750
1.0	B	12208	11362
1.0	C	8615	
2.0	A	3761	
2.0	B	16952	
2.0	C	4333	

The plate properties and dimensions are

Membrane Layers	Distance to Neutral Surface (inches)	Thickness (inches)	Modulus of Elasticity (psi)	Poisson's Ratio
1	.486	.050	30×10^6	.3
2	.223	.075	10×10^6	.3
3	.114	.100	10×10^6	.3
4	.494	.060	30×10^6	.3

Core Layers	Distance to Centroid (inches)	Thickness (inches)	Shear Moduli (psi)
1	.362	.200	10000
2	.062	.250	8000
3	.312	.200	12000

Ly = 100 inches

Lx varies from 40 inches to 200 inches.

The results of loading the plate with a uniformly distributed uniaxial stress in the x-direction are plotted in Figure 15 for both a 4 x 4 and an 8 x 8 grid.

To further demonstrate the method the critical stress for the first mode of a plate with the same cross-sectional properties is determined for the support conditions shown in Figure 16. The resulting critical stress for the first mode is 26102 psi.

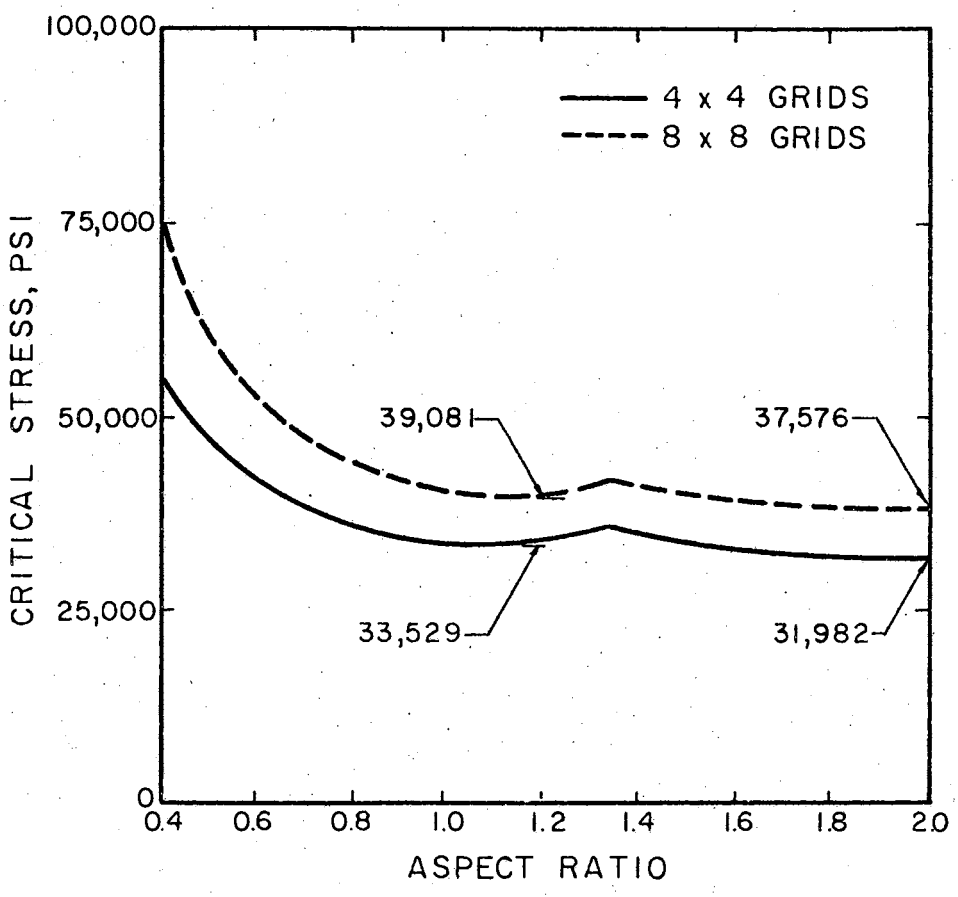

Figure 15. Critical Stresses for Simply Supported Rectangular Multilayer Plate

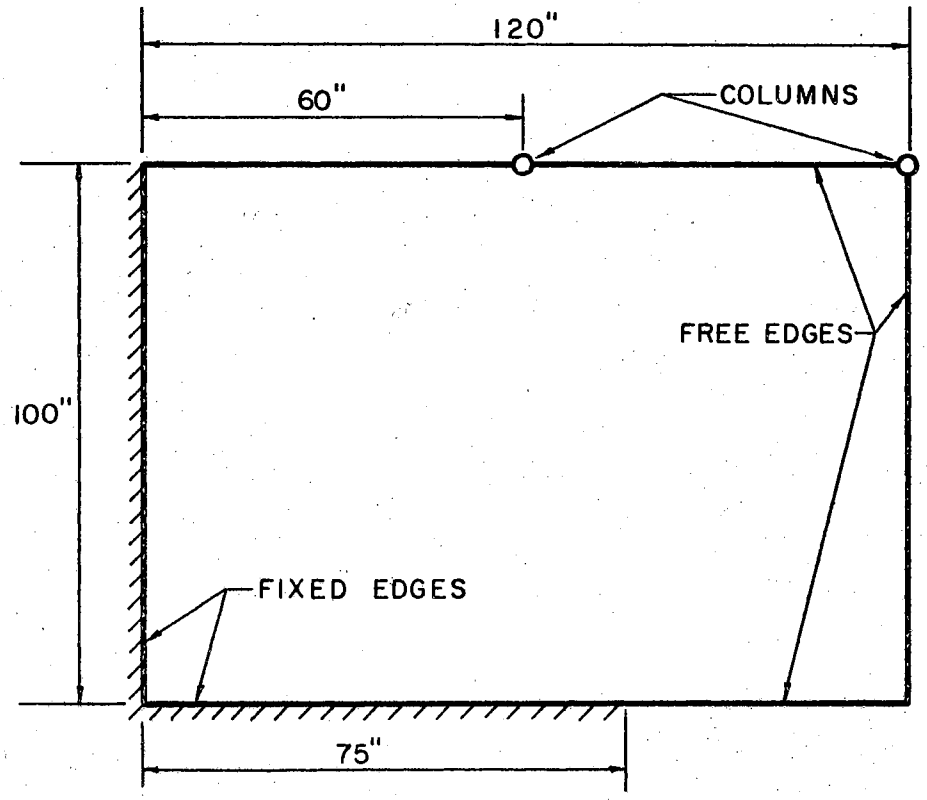

Figure 16. Support Conditions for Multilayer Plate Problem

CHAPTER XII

SUMMARY AND CONCLUSIONS

7.1 Summary

A method for determining the critical buckling load of multilayer sandwich plates has been developed in this thesis. The method consists of the application of the finite element method to layered plates. It provides for approximate solutions to three layered sandwich plates whose boundary conditions can not be accommodated by existing analytical methods as well as solutions of multilayer sandwich plates.

The material property assumptions made are consistent with experimental investigation of sandwich construction. The solution is based upon small deflection theory of thin plates and therefore is not applicable in the case of thick or flexible plates. Also, the bending stiffness of the individual membrane layers is neglected, therefore plates with thick membrane layers would not yield dependable results.

The weighted neutral surface concept (7) allows the bending properties of the layered section to be treated as an equivalent homogeneous section.

Stress functions were assumed in developing both the bending and in-plane stiffnesses. The functions used are of higher order than those previously utilized for homogeneous plates in order to provide more accurate representation of the shearing deformation.

A displacement function was assumed for determining the stiffness modifier because the formulation seemed to be much more direct.

Theoretically it appears that the stress function should give better results than a displacement function (15). There has not yet been enough comparative work done to conclude that it is always so.

The vertical component of the in-plane forces due to displacement has been neglected because of it's higher order. Also, it is felt that its inclusion would require a more complex solution procedure and therefore negate some of the advantages of the method.

The analytical use of the magnification procedure provides a quickly converging method of determining the critical stresses for the low modes. Eigenvalue solutions are available, however, to which the stiffness matrices developed in this thesis may be applied when the critical stresses for higher modes are desired (17, 18).

7.2 Discussion of Results

Where other solutions are available for comparison, results appear to be quite good. It is somewhat difficult to conclude conclusively because most of the existing solutions are also approximate.

For the uniaxially loaded homogeneous plate problems worked, the largest deviation from the existing solution is 13%. The next largest deviation is 6.0%. The mean deviation is 1.6%. It should be noted that both the high deviations are for modes greater than the first. This same trend was noticed in sandwich plate results. However, some excellent agreement was found in higher mode solutions. Another characteristic is noticeable. The Type C boundary condition tends to produce greater deviation from existing results than Type B. This is

surprising since Type C deformation conforms more closely to the assumed double sine series than does Type B.

The deviations for homogeneous biaxially loaded plates run slightly greater. The mean is 2.7%.

For the uniaxially loaded sandwich plates the mean deviation is 5.5%.

The curves plotted for the multilayer plate take on the same characteristics as homogeneous plates.

The solution, as a function of grid size, converges from below. There are not any tabulations of critical stress computations of multilayer plates although methods for analysis of simple support conditions have been developed in two papers (7, 8).

The multilayer problem with fixed support on a portion of one edge and two column supports described in Figure 15 has been included to demonstrate the capacity of the method to accommodate irregular support conditions.

7.3 Conclusions

The results have demonstrated that the method of finite elements can provide solutions of reasonably good accuracy for sandwich plate critical stress problems. Some experimental results are needed to fully evaluate the usefulness of the technique, since rigorous solutions are sparse.

It should be noted that the grid used here is relatively course. It is believed that a finer grid should be used if dependable results are to be expected from plates with irregular support conditions.

The mechanics of the method allows plates with holes or irregular

boundaries to be solved. However, a fine grid is again indicated and more corroborative work needs to be done.

The magnification method utilized to determine the critical stress has been successful with some reservations. In addition to the discussion within the text relative to obtaining higher modes, several pertinent facets of the method should be mentioned. The prediction factor is based upon the assumption of a sine wave shaped displacement. It has been shown in this thesis that it yields good results for displacement configurations that are not especially close to a sine curve. This does not, of course, mean that good convergence will occur for all mode shapes. One advantage of the magnification method as compared to an eigenvalue solution is that by controlled iteration the deformation response of the plate can be examined.

The solutions presented in Chapter VI used a set of stress functions containing twenty-seven independent coefficients. Stress functions with seven and with seventeen independent coefficients were formulated but were not used because they reflected only constant and linear, respectively, variation of the transverse shear stresses. For problems where the transverse shear stress is not deemed important, the full twenty-seven term expressions would probably not be necessary.

The results of this thesis and the similarity of problem characteristics lead to vibration analysis of sandwich plates as a natural sequential step in the application of the method of finite elements. Studies in elasto-plastic behavior appear to also be possible.

BIBLIOGRAPHY

(1) Reissner, E., "On Bending of Elastic Plates." Quar. Appl. Math., Vol. 5, 1947, pp. 55-68.

(2) Reissner, E., "Finite Deflections of Sandwich Plates." Jour. Aero. Sci., Vol. 15, 1948, pp. 435-440.

(3) Hoff, N. J., "Bending and Buckling of Rectangular Sandwich Plates." NACA Tech. Note 2225, 1950.

(4) Eringen, A. C., "Bending and Buckling of Rectangular Sandwich Plates." Proc., First U. S. Nat. Cong. Appl. Mech., 1951, pp. 381-390.

(5) Kuenzi, E. W., C. B. Norris, and P. M. Jenkinson, "Buckling Coefficients for Simply Supported and Clamped Flat, Rectangular Sandwich Panels Under Edgewise Compression." U. S. Forest Service Research Note, FPL-070, 1964.

(6) Liaw, B. D., "Theory of Bending of Multilayer Sandwich Plates." Ph. D. Thesis, Oklahoma State University, Stillwater, Oklahoma, 1965.

(7) Wong, J. P., "Stability of Multilayer Sandwich Plates." Ph. D. Thesis, Oklahoma State University, Stillwater, Oklahoma, 1966.

(8) Pomazi, L. P., "On the Stability of Multilayer Plates." Izv. VUZ, Mashinostr., No. 2, 1966, pp. 29-34.

(9) Bolotin, V. V., "On the Reduction of Three-dimensional Problems of Elastic Stability to One and Two-dimensional Problems." Sb. "Stability Problems in Structural Mechanics." Stroiizdat, 1965.

(10) Turner, M. J., R. W. Clough, H. C. Martin, and L. J. Topp, "Stiffness and Deflection Analysis of Complex Structures." Jour. Aero. Sciences, Vol. 23, 1956.

(11) Melosh, R. J., "A Stiffness Matrix for the Analysis of Thin Plates in Bending." Jour. Aero. Sci., 28, 1961, pp. 34-43.

(12) Melosh, R. J., "Basis for Derivation of Matrices for the Direct Stiffness Method." Amer. Inst. Aero. Astro. Jour., Vol. 1, No. 7, 1963, pp. 1631-1637.

(13) Best, G. C., "A General Formula for Stiffness Matrices of Structural Elements." Amer. Inst. Aero. Astro. Jour., Vol. 1, No. 8, 1963, pp. 1920-1921.

(14) Pian, T. H. H., "Derivation of Element Stiffness Matrices." Amer. Inst. Aero. Astro. Jour., Vol. 2, No. 3, 1964, pp. 576-577.

(15) Pian, T. H. H., "Derivation of Element Stiffness Matrices by Assumed Stress Distributions." Amer. Inst. Aero. Astro. Jour., Tech. Notes, Vol. 2, No. 7, 1964, pp. 1333-1336.

(16) Zienkiewicz, O. C., and T. K. Cheung, "The Finite Element Method for Analysis of Elastic Isotropic and Orthotropic Slabs." Proc. Instn. Civ. Engrs., Vol. 28, 1964, pp. 471-488.

(17) Severn, R. T. and P. R. Taylor, "The Finite Element Method for Flexure of Slabs when Stress Distributions are Assumed." Proc. Instn. Civ. Engrs., Vol. 34, 1966, pp. 153-170.

(18) Timoshenko, S. F. and J. M. Gere, Theory of Elastic Stability. 2nd Ed. McGraw-Hill Book Co., Inc., New York, 1961.

(19) Hartz, B. J., "Matrix Formulation of Structural Stability Problems." Proc. Amer. Soc. Civ. Engrs., Struc. Jour., Dec. 1965, pp. 141-157.

(20) Kapur, K. K. and B. J. Hartz, "Stability of Plates Using the Finite Element Method." Proc. Amer. Soc. Civ. Engrs., Struct. Jour., April 1966, pp. 177-195.

(21) Bolotin, V. V., The Dynamic Stability of Elastic Systems, Holden-Day, Inc., San Francisco, 1964.

(22) Gallagher, R. H. and J. Padlog, "Discrete Element Approach to Structural Instability Analysis." Amer. Inst. Aero. Astro., Vol. 1, No. 6, 1963, pp. 1437-1439.

(23) Archer, J. S., "Consistent Matrix Formulations for Structural Analysis Using Finite-Element Techniques." Amer. Inst. Aero. Astro., Vol. 3, No. 10, 1965, pp. 1910-1918.

(24) Southwell, R. V., "On the Analysis of Experimental Observations in Problems of Elastic Stability." Proc. Roy. Soc. (London), Ser. A, Vol. 135, 1932, pp. 601-616.

(25) Gerard, G., Introduction to Structural Stability Theory. McGraw-Hill Book Co., Inc., New York, 1962.

(26) Plantema, F. J., Sandwich Construction. John Wiley and Sons, New York, 1966.

APPENDIX A

COMPUTER PROGRAM BLOCK DIAGRAM

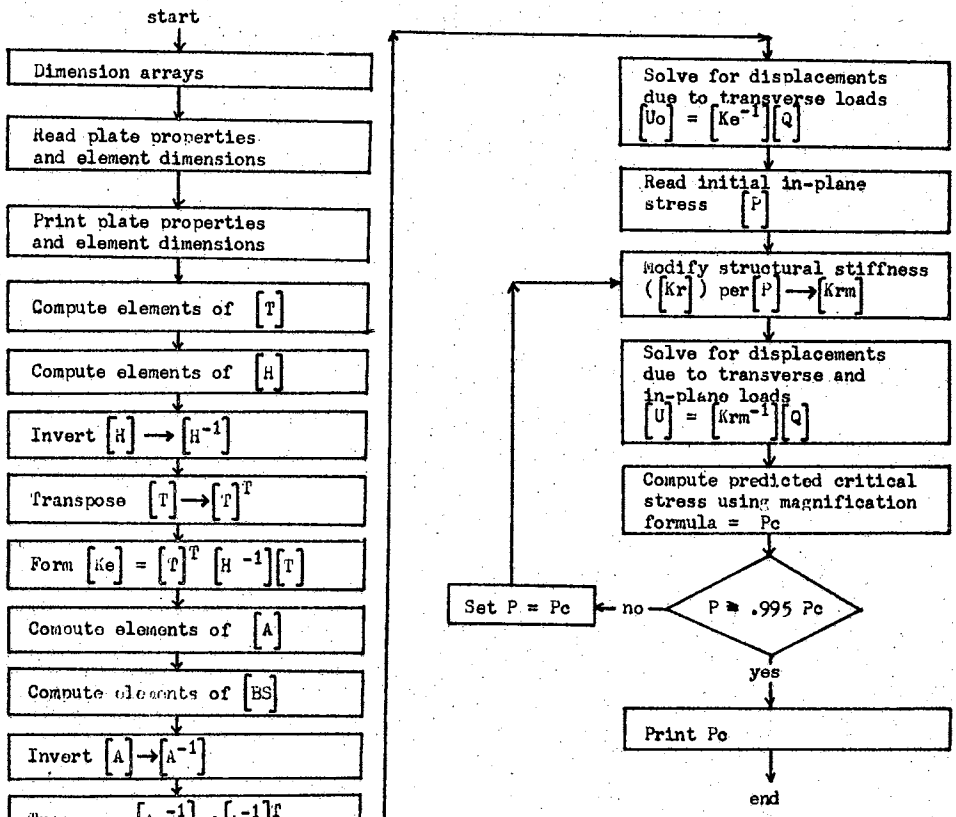

VITA

Harry Richard Lundgren

Candidate for the Degree of

Doctor of Philosophy

Thesis: BUCKLING OF MULTILAYER PLATES BY FINITE ELEMENTS

Major Field: Engineering

Biographical:

Personal Data: Born May 2, 1928, in Chicago, Illinois.

Education: Graduated from Crown Point High School, Crown Point, Indiana, in June, 1946. Received the Bachelor of Science in Civil Engineering, Purdue University, West Lafayette, Indiana, in June, 1950. Received the Master of Science of Engineering, Arizona State University, Tempe, Arizona, May, 1962.

Professional Experience: Design Engineer and Project Engineer for The Kawneer Company, Niles, Michigan, 1953-1958. Vice-President of Engineering, R. B. Feffer and Sons, Phoenix, Arizona, 1958-1959. Civil Engineer, Salt River Project, Phoenix, Arizona, 1959-1961. Graduate Assistant, Instructor, and Assistant Professor, Arizona State University, 1961-1967. Member of ASCE, N.S.P.E., A.S.E.E., and Arizona Society of Structural Engineers. Registered Civil and Structural Engineer in Arizona.